PHYSICAL REVIEW B VOLUME 31, NUMBER 10 15 MAY 1985

Frustration, curvature, and defect lines in metallic glasses and the cholesteric blue phase

James P. Sethna
Institute for Theoretical Physics, University of California, Santa Barbara, Santa Barbara, California 93106
*and Laboratory of Atomic and Solid State Physics, Cornell University, Ithaca, New York, 14853**
(Received 24 September 1984)

We develop continuum elastic theories for the blue phases of cholesteric liquid crystals and for the metallic glasses. These theories are frustrated and possess ground states with networks of defect lines; the frustration can be relieved in a space of constant positive curvature (a sphere in four dimensions). The order parameter for the blue phase is a director (in $\mathbb{R}P^2$), and for the metallic glasses it is a 4×4 rotation matrix [in SO(4)]. The elastic energies are written using covariant derivatives which are zero for the local low-energy configurations. The theories are nonlinear sigma models. We also develop a renormalization-group analysis of disclination cores in models with $\mathbb{R}P^2$, vector, SO(3), and SO(4) order-parameter spaces. The energy of disclination lines diverges logarithmically as their core size is taken to zero. A total divergence can be added to the energy. Through an unusual combination of energetic and topological effects, it contributes an energy proportional to the product of the length and strengths of the disclinations. We use this total divergence as a counterterm to keep the disclination energies fixed in the continuum limit.

I. INTRODUCTION

Several condensed-matter systems have stable phases possessing networks of defect lines. Cholesteric fluids can have several "blue phases" in a small temperature region between the helical and isotropic phases;[1] these phases have been described as networks of $-180°$ disclination lines.[2,3] Transition-metal alloys have several Frank-Kasper phases;[4] these and the metallic glasses have been described as networks of $-72°$ disclinations.[5,6] The smectic-D phase[7] and a similar phase of lipid-water systems[8] have water confined in an elaborate network of tubes. Finally, rotating superfluids and type-II superconductors in magnetic fields have (two-dimensional) lattices of vortex lines.[9]

In this paper we develop exotic continuum field theories to describe the first two of these systems. The director theory of the blue phases was outlined in a paper several years ago;[2] the continuum theory for metallic glasses was outlined in a short early version of this work.[10] Other continuum theories (with more complicated order parameters) have been developed both for the blue phases[11,12,1] and for the metallic glasses.[13] Many of the ideas developed here (in particular the construction of the covariant derivatives) also apply to those theories.

These substances are frustrated: No configuration can relax the strain energy completely. In Sec. II we will describe this frustration in detail, and show how the defect lines can act to relieve it. The frustration disappears if one (formally) curves space onto a sphere in four dimensions.[14–17] In Sec. III we describe the ideal unstrained structure formed on this sphere. In Sec. IV we use these ideal templates to form order parameters describing the phases.

In Sec. V we construct the continuum theories. The local low-energy field configurations (projections from the ideal template) cannot be used to fill space. To construct frustrated free energies, we form covariant derivatives which are zero for the ideal configurations. The covariant derivatives will have a nonzero curvature; the curvature represents the frustration in the natural parallel transport. The resulting theories are nonlinear sigma models which (renormalized properly) have ground states possessing networks of disclination lines.

The continuum limit in these theories is subtle. On the one hand, the energy of disclination lines diverges logarithmically as the core size is taken to zero. On the other hand, the core size in the real materials is comparable to the interdefect spacing. (The atomic size is comparable to the distance between defects in metallic glasses and the Frank-Kasper phases; the coherence length must be comparable to the pitch for the blue phases to be stable.[12,2])

In Sec. VI we give a renormalization-group analysis of the continuum limit in these two theories. We use a total divergence term in the free energy as a counterterm. It acts as a surface energy, leaving the bulk behavior unchanged but altering the energetics of the disclination lines. Through an unusual combination of energetic and topological effects, the total divergence term changes the energy per unit length by an amount precisely proportional to the strength of the disclination. By allowing the magnitude of the counterterm to diverge as the core size goes to zero, we can keep the energy of the disclination lines fixed.

Thus we claim that the continuum theories developed here are in the same universality class as the materials they model. In consequence, despite the uncontrolled approximation of ignoring the core size, any properties which are preserved in the continuum limit will be universal, and independent of the model. For example, properties of (hypothetical) defect-mediated phase transitions in these models might explain the commonly accepted phenomenology of the glass transition.[18] As emphasized by Nelson,[19] the problem of defect entanglement may be

crucial in understanding metallic glasses. Viscous flow, for example, could occur after a phase transition at which the disclination energy per unit length vanishes.

II. FRUSTRATION, LOCAL ORDER, AND DEFECT LINES

The term frustration was introduced by Toulouse in the study of spin glasses.[20] Spin glasses are modeled, for example, by Ising spins on a lattice with the nearest-neighbor bonds in the Hamiltonian chosen at random to be ferromagnetic or antiferromagnetic. The low-energy spin configurations will satisfy as many of these bonds as possible. Frustration expresses the spatial competition between these bonds. Consider moving around a closed loop (Fig. 1). The state of the first spin is arbitrary; the state of each succeeding spin can be chosen in turn to satisfy the bond preceding it on the path. If there are an odd number of antiferromagnetic bonds in the loop, this "parallel transport" will leave the last bond in its high-energy state. Parallel transport is defined by minimizing the energy locally as one moves around the path; when parallel transport does not return to its initial value, the loop is said to be frustrated.

Systems can be frustrated without including disorder explicitly in the Hamiltonian. Consider parallel transport of vectors on a sphere. Imagine a physical substance on the surface which is described at each point by a unit vector tangent to the sphere, e.g., a two-dimensional XY ferromagnet or a two-dimensional nematic liquid crystal. Suppose the free energy contains gradient terms which are minimized locally by having the tangent vectors all point in the same direction. Although one can do this along a narrow path (defining a parallel transport), one cannot make these gradient terms vanish in a region of finite area. When a path crosses itself forming a loop, there will in general be a change in the direction of the vector, and for small loops this change will be proportional to the area enclosed (Fig. 2). The frustration represented by this change in direction is described by the curvature tensor $\mathscr{R}$ of the sphere: If one parallel transports a vector $\mathbf{v}$ along a small parallelogram with sides $\mathbf{x}$ and $\mathbf{y}$, the change $\delta\mathbf{v}$ in $\mathbf{v}$ is given by

$$\delta v^i = \mathscr{R}^i{}_{jkl} v^j x^k y^l . \tag{2.1}$$

For the sphere of radius κ^{-1}, if θ and ϕ measure latitude and longitude, respectively, then for example $\mathscr{R}^{\theta}{}_{\phi\theta\phi} = \sin^2\theta$; contraction with the metric tensor gives a scalar curvature of $2\kappa^2$.[21]

The two systems discussed in this paper—metallic glasses and the blue phase—have no intrinsic disorder in their Hamiltonians. Like the two-dimensional nematic liquid crystal on the sphere, the models we will use for these systems are uniformly frustrated, and many of the tools developed in differential geometry to study curved surfaces will be useful to us. In this section we shall motivate these models by giving a microscopic physical description of frustration in these two systems. We start by describing frustration in metallic glasses, and how defect lines can be used to relieve the frustration. We then turn to the cholesteric blue phases.

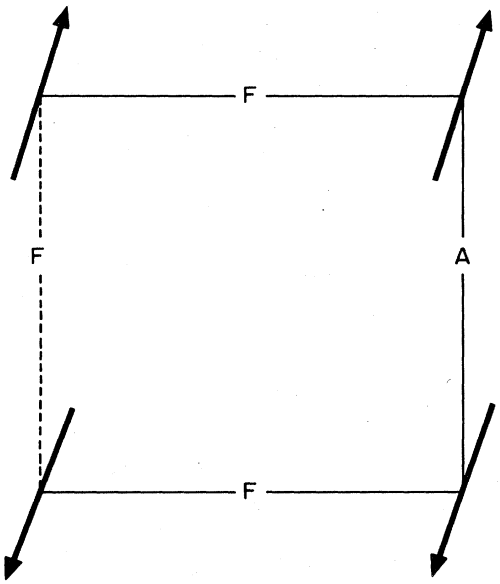

FIG. 1. *Frustration in spin glasses.* The bonds of an Ising spin glass are fixed random quantities, which either favor parallel (ferromagnetic) or opposing (antiferromagnetic) spins. The spins point either up or down, and are free to relax the bond energies; however, some residual energy is unavoidable. In this figure, we satisfy each bond in turn clockwise starting from the upper left. Because there are an odd number of antiferromagnetic bonds, the last bond is in its high-energy state—the loop is frustrated.

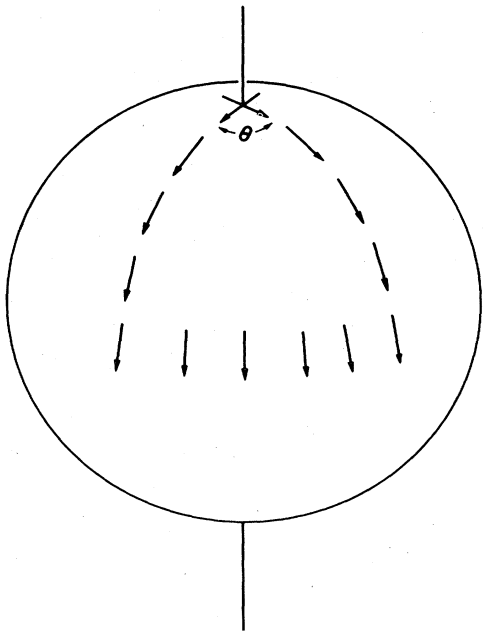

FIG. 2. *Frustration on a sphere.* An XY ferromagnet is frustrated on the surface of a sphere in three dimensions. We define a parallel transport, minimizing the energy locally along a path. Parallel transport here from the pole to the equator, along the equator an angle θ and back to the pole rotates the order parameter an angle θ.

We shall think of the metallic glasses as a collection of identical atoms interacting via soft pair potentials.[22] Although this may be a good description for solid argon, it is a very simplified model for metallic glasses. (Argon, although it forms amorphous clusters of 500—1000 atoms,[23] does not have interesting bulk phases.) Metallic glasses typically are made with two types of atoms—a transition or noble metal and a metalloid.[24] The stability of the metallic glass is strongly dependent on the ratio of metal to metalloid. We ignore these features of the real system;[25] we also ignore bond directionality and the effects of the electrons on the structural properties.[26] In this simplification, we hope we are isolating the important features of the metallic glasses from the complexities of the real system.

In two dimensions, systems of interacting disks naturally form hexagonal arrays of equilateral triangles. Each atom is surrounded by six neighbors; the nearest-neighbor separation is roughly the minimum of the pair potential. In three dimensions, four atoms can form a local low-energy tetrahedral cluster (Fig. 3), with each pair of atoms at the pair potential minimum. Adding a fifth atom will form a second tetrahedron, but this cannot be continued to fill space with tetrahedra. In Fig. 4, we see five tetrahedra sharing an edge. Since the opening angle at the edge of a tetrahedron does not divide 360°, there is a 7.5° gap between two of the tetrahedra. One has a choice of closing this gap by stretching the five tetrahedra slightly, or squeezing them to add a sixth. [The fivefold-coordinated edges will have a lower strain energy; however, one must introduce sixfold coordinated edges ("6-lines") to build a lattice. Strains introduced in making a cluster purely out of fivefold lines grow rapidly with the radius: The sixfold lines are necessary to relax these strains.] Nelson[6] has introduced the idea that the high-strain 6-lines should be thought of as defect lines in an ideal structure of fivefold coordinated edges.

Closest packing structures (fcc and hcp) are not naturally described in terms of tetrahedra and defect lines. Because of the symmetries of the crystals, octahedra are formed which have more than one equivalent decomposition into tetrahedra (Fig. 5). While every atom in a closest packing structure has twelve neighbors, Frank[27] has shown in a precise way that these structures do not locally minimize the energy. He showed that an icosahedral cluster of thirteen atoms (one atom plus its twelve neighbors) interacting via soft pair potentials has a significantly lower energy than the nearest-neighbor cluster in fcc and hcp crystals. This icosahedral cluster can be visualized as twenty slightly distorted tetrahedra meeting at a vertex. Thus we can visualize the local low-energy structure ei-

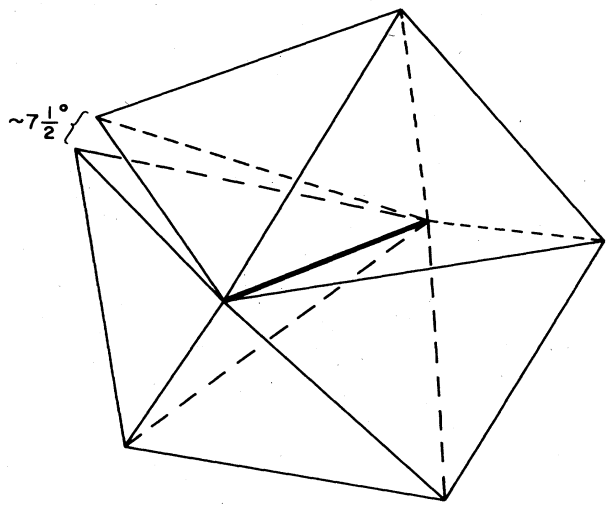

FIG. 4. *Frustration in metallic glasses.* One cannot fill space with undistorted tetrahedra. Five tetrahedra will fit around an edge, leaving a gap of about $7\frac{1}{2}°$. Curvature can remove this frustration; the circle formed by the five outer atoms would have a smaller circumference for fixed radius in a space of positive curvature.

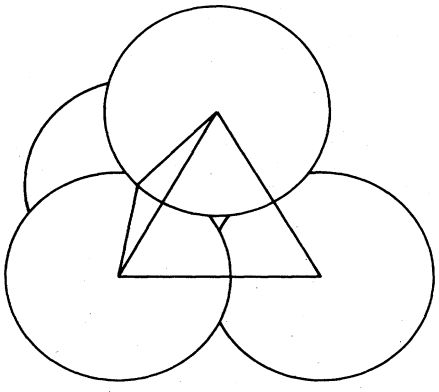

FIG. 3. *Metallic glass tetrahedral cluster.* The natural local low-energy structure in metallic glasses is a tetrahedral cluster of four atoms.

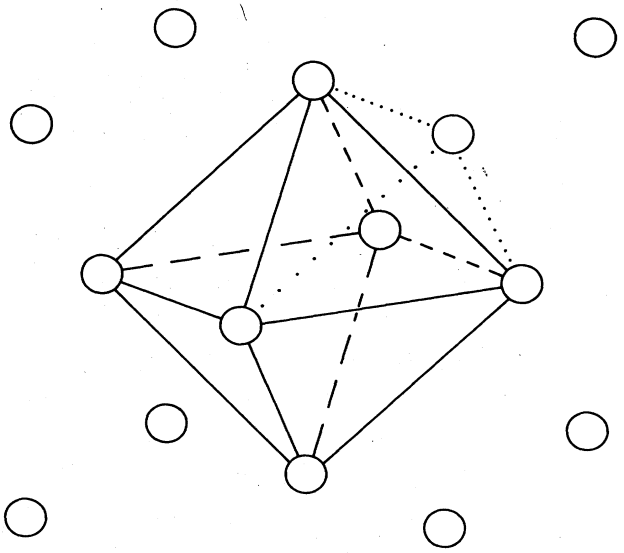

FIG. 5. *Closest packing structures contain octahedra.* The unit cell of the face-centered cubic structure shown here contains two octahedra and eight tetrahedra.

ther in terms of tetrahedra of four atoms or in terms of icosahedra of thirteen; our ideal template in the next section will combine both features.

There are a number of transition-metal alloys which, unlike the closest packing structures, have natural descriptions as networks of 6-lines.[6] The description of these Frank-Kasper[4] phases was originally motivated by low-energy icosahedral cluster described above. They have large unit cells, with up to 162 atoms. The $A15$ compounds (e.g., Nb_3Sn) are the simplest, with eight atoms per cell (Fig. 6); the sixfold coordinated edges form straight lines running in three orthogonal directions, connecting the niobium atoms. The tin atoms sit at the center and the corner of the unit cell, with twelve niobium neighbors forming a distorted icosahedron surrounding the center. We interpret the Frank-Kasper phases as a natural way of relieving frustration by introducing a regular pattern of defect lines. The defect lines will form an irregular pattern in the metallic glasses.

Cholesteric fluids are composed of long, thin chiral molecules,[28] typically 5 Å × 50 Å. That is, the molecules have a handedness—they differ from their mirror image. A pair of neighboring cholesteric molecules will have minimum energy when they sit at a very slight angle with respect to each other. One can understand this angle by visualizing screw threads on the surface of the molecules (Fig. 7). (Commercial screws are right-handed.) To align the threads on the back of one molecule with the grooves on the front of the next, the rear molecule must be twisted slightly to the right. The twist angle is very small; the cholesteric pitch (the distance required to build up a 360° rotation) is hundreds or thousands of angstroms. In the phases of interest to us we may ignore the azimuthal orientations of the molecule about its axis, and the distinction between the ends of the molecule: We describe the orientation of a molecule by a headless unit vector or "director" $\vec{n}$.

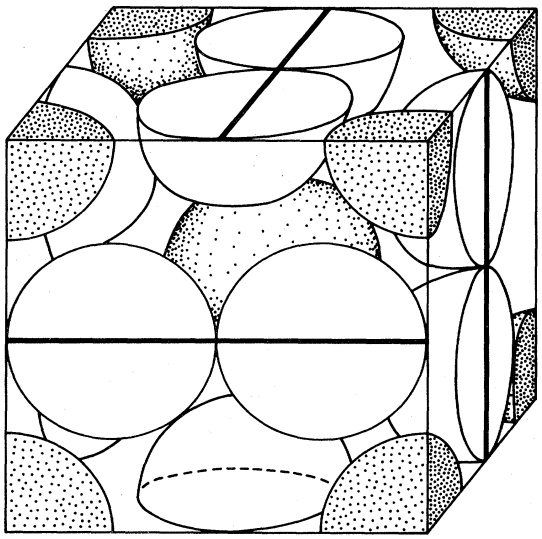

FIG. 6. *Frank-Kasper phases are networks of defect lines.* Here is shown the unit cell for an $A15$ compound, say Nb_3Sn. Tin atoms are grey, niobium white. 12 niobium atoms form a distorted icosahedron around each tin atom. Ten niobium atoms and four tin atoms surround each niobium; a sixfold coordinated edge passes through each niobium atom. These defect lines form the rectangular array shown.

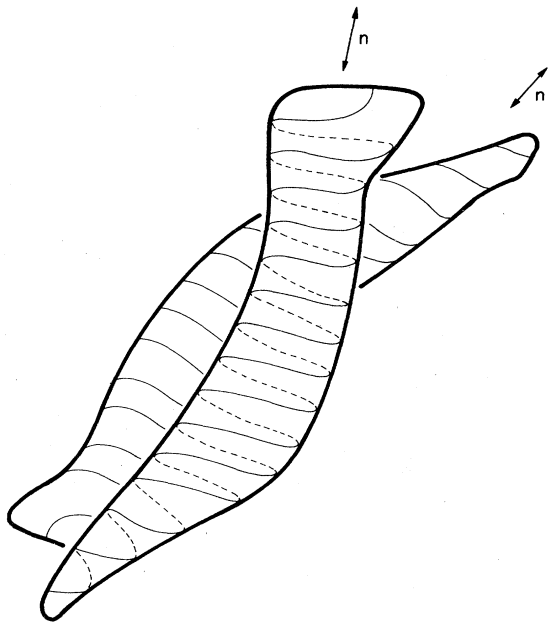

FIG. 7. *Neighboring cholesteric molecules sit at a slight angle.* Because the molecules are chiral, the pair interaction energy between two molecules in a cholesteric is minimized when they are slightly misaligned. Here the forward molecule is twisted slightly counterclockwise (a right-handed twist).

Consider now a small region of cholesteric fluid, in a local low-energy state. As one moves radially outward from a central molecule, the molecular orientations will gradually twist to the right (Fig. 8); as one moves along the axis of the molecule the orientations will not change (by symmetry). In general, the change in orientation of the molecule is perpendicular both to the direction of

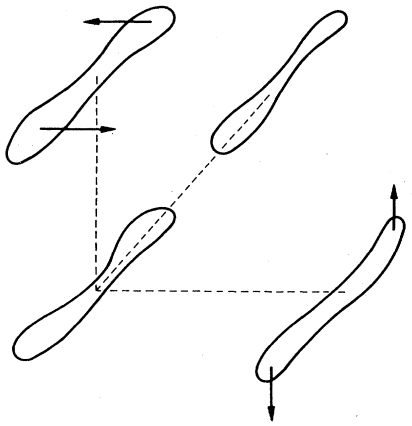

FIG. 8. *Parallel transport in cholesterics.* As one moves radially outward, the low energy orientation spirals to the right; as one moves along the molecular axis the orientation is unchanged.

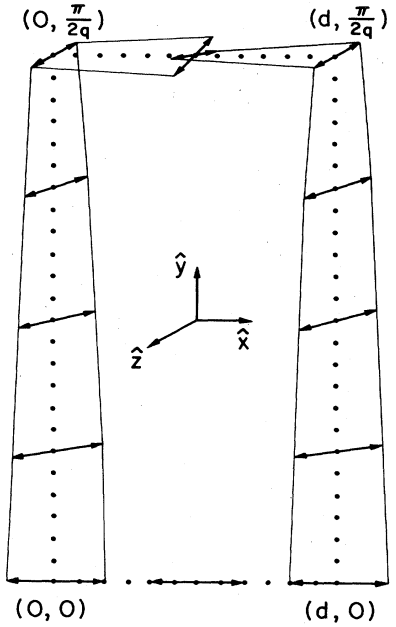

FIG. 9. *Frustration in the blue phase.* Parallel transport in cholesterics is frustrated. The local low-energy condition (2.2) for cholesteric fluids cannot be everywhere satisfied. Consider the closed loop above. Start with a director $\vec{n}$ at the origin pointing in the $\hat{x}$ direction. As we move in the $\hat{y}$ direction, (2.2) dictates that $\vec{n}$ rotate, until at $(0,\pi/2q)$ it lies in the $\hat{z}$ direction. Along the $\hat{x}$ axis, the low-energy state allows the direction of $\vec{n}$ to remain unchanged; thus if we parallel transport $\vec{n}$ using (2.2) first to $(d,0)$ and then to $(d,\pi/2q)$, $\vec{n}$ will again point in the $\hat{z}$ direction. Finally, if we transport these two to meet at $(d/2,\pi/2q)$, they will point in different directions, with angular separation dq.

motion and to the molecule; the local low-energy configuration satisfies[2,3]

$$\partial_i n_j = -q\epsilon_{ijk} n_k \ , \tag{2.2}$$

where $2\pi/q$ is the cholesteric pitch and ϵ_{ijk} is totally antisymmetric in its indices with $\epsilon_{123}=1$.

Cholesteric fluids are frustrated; it is not possible to satisfy the energy minimization condition (2.2) in any finite volume. This can be seen by considering parallel transport around an infinitesimal closed loop. (Figure 9 discusses transport around a larger loop.) If one moves an infinitesimal distance **a**, then a distance **b**, then back along $-\mathbf{a}$ and $-\mathbf{b}$, changing $\vec{n}$ to satisfy (2.2) along the path, then $\vec{n}$ will in general be rotated to a new vector $\vec{n}'$, given to lowest order in **a** and **b** by

$$\begin{aligned} n_i' &= n_i - \mathscr{R}_{ijkl} a_k b_l n_j \\ &= n_i - q^2(\delta_{jk}\delta_{il} - \delta_{lj}\delta_{ik}) a_k b_l n_j \ . \end{aligned} \tag{2.3}$$

Thus in particular, an ideal low-energy state would have

$$\partial_l \partial_k n_i - \partial_k \partial_l n_i = q^2(\delta_{il} n_k - \delta_{ik} n_l) \neq 0 \ .$$

The tensor $\mathscr{R}_{ijkl}$ is the analog of the curvature tensor in differential geometry, and of the field strength tensor $F^{\mu}{}_{\nu}$ in gauge theories. One can contract it to form a scalar "curvature,"

$$\mathscr{R}_{ijij} = -6q^2 \ , \tag{2.4}$$

which is negative. We shall see in Sec. III that by working on a space of positive (metric) curvature (a sphere in four dimensions), we can make this frustration disappear.

[In differential geometry, parallel transport can be defined on a curved manifold using the connection coefficients $\Gamma^i{}_{jk}$.[29] If one assumes that the connection is symmetric ($\Gamma^i{}_{jk} = \Gamma^i{}_{kj}$), these coefficients can be written solely in terms of the metric and its gradients, and thus are uniquely defined by the manifold. This is normally a sensible assumption, and the curvature of the connection equals the curvature of the space. In condensed-matter physics, space is flat; however, in cholesteric fluids, the connection $\Gamma^i{}_{jk} = q\epsilon_{ijk}$ is not symmetric and the curvature of the connection is negative. The asymmetry is the torsion tensor $T^i{}_{jk} = \frac{1}{2}(\Gamma^i{}_{jk} - \Gamma^i{}_{kj}) = q\epsilon_{ijk}$.]

At low temperatures, cholesteric fluids have a helical phase (Fig. 10), of the form

$$n(x) = \hat{x}\cos(qz) + \hat{y}\sin(qz) \ . \tag{2.5}$$

This phase does not satisfy the double-twist condition (2.2). It twists in only one of the two directions perpendicular to $\vec{n}$, and locally is not the lowest-energy state. The minimum-energy double-twist state can be achieved in the center of a tube (Fig. 11):

$$n(x) = \hat{z}\cos(qr) - \hat{\theta}\sin(qr) \ . \tag{2.6}$$

The energy density at the center of this tube will be substantially lower than that of the helical phase. (Note that *right*-handed molecules, Fig. 7, produce *left*-handed tubes, Fig. 11. That is, molecules with threads spiraling to the right will orient themselves on a low-radius tube so as to form lines spiraling to the left.) The energy density grows with radius; strains build up as the double-twist relation must be violated more and more. By the time $n = -\hat{\theta}$ (90° tubes) the molecules twist only in the $\hat{r}$ direction, while they bend in the $\hat{\theta}$ direction: The energy density has

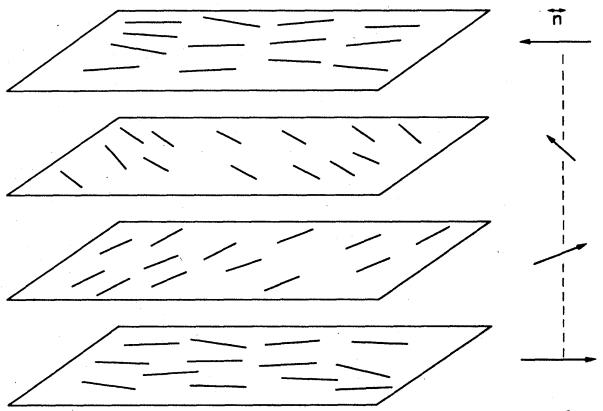

FIG. 10. *Low-temperature cholesteric phase twists in one direction.* (The planes are to aid visualization; there is no density variation in the vertical direction.)

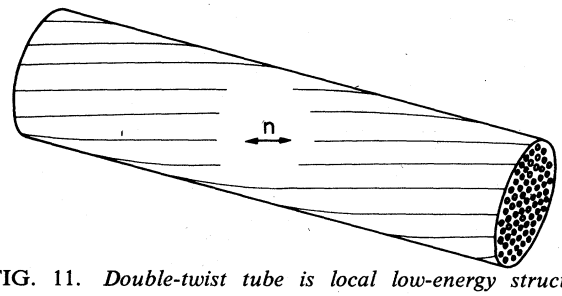

FIG. 11. *Double-twist tube is local low-energy structure.* Along the center line of the cylinder the cholesteric free energy is minimized; moving radially outward the energy density increases.

risen above that of the spiral phase. (See also Finn and Cladis,[30] whose "cholesteric sphere of positive sign" can be generated by parallel transport radially outward from a center.)

We shall build model blue phases out of double-twist tubes. Two 45° tubes will naturally sit at right angles. (If the molecules on the surface of a tube are aligned at an angle θ with respect to the axis, then two tubes will align at an angle 2θ to keep the molecular orientation continuous at the point of tangency. See, e.g., Fig. 7 depicting the similar behavior of two molecules with threads.) Three such tubes can form a corner; this corner can be either right-handed [(Fig. 12(a)] or left-handed [Fig. 12(b)]. If the cholesteric pitch is right-handed ($q > 0$, as shown in the figure), then the left-handed corners (b) contain no singularity; fluid can fill the region between the tubes, smoothly pointing out of the corner. Right-handed corners (a) must contain a topological singularity, as the director rotates 180° along a closed path on the surfaces of the cylinders enclosing the corner.

The singularity contained by right-handed corners is an $s = -\frac{1}{2}$ disclination line (Fig. 13). These lines are characteristic of the blue phases. They relax the frustration imposed by the double twist the same way 6-lines relax strains in the metallic glasses.

Experimentally,[1] the blue phases occupy a small ($\sim$1-K) temperature range between the isotropic phase and the spiral phase. (The small temperature range can be explained in terms of the energetics of defect lines.[2] At low temperatures you spend more energy in the "isotropic" core of the defect than you gain from the regions of double twist.) Up to three phases can appear in a given material. The two lower temperature phases are crystalline; blue phase I has a bcc translation group and blue phase II is simple cubic. The lattice constants (roughly the cholesteric pitch) are wavelengths of the blue light—Bragg reflections cause the brilliant colors. The high-temperature phase, the "blue fog," is amorphous (no

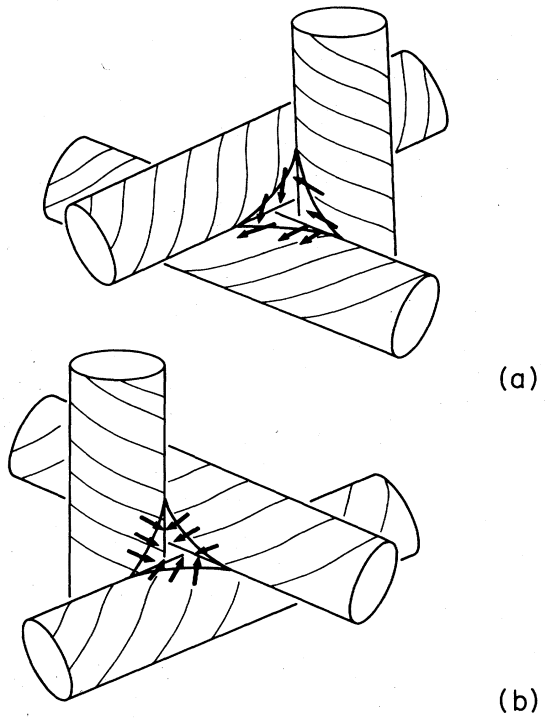

FIG. 12. (a) *Right-handed corners contain* $s = -\frac{1}{2}$ *defect lines.* Three double-twist tubes forming a right-handed corner. Note that the director rotates 180° as one moves in a closed path around the corner. There is no way to fill the corner smoothly with directors. (b) *Left-handed corners have no singularity.* Three double-twist tubes in a right-handed cholesteric forming a left-handed corner. Note that the director rotates 360° as one moves around the corner. The corner can be filled smoothly with arrows pointing into the paper.

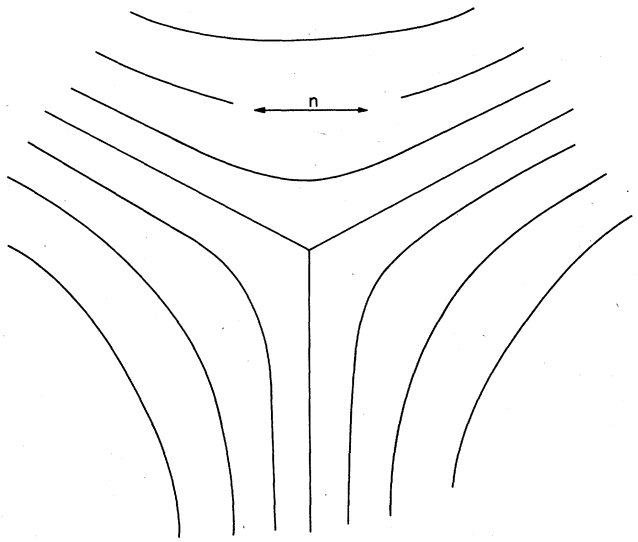

FIG. 13. $s = -\frac{1}{2}$ *disclination line.* Cross section of a $s = -\frac{1}{2}$ disclination line. The director order parameter $\vec{n}$ lies tangent to the curves in the figure. As one travels around the defect n rotates backward halfway (−180°).

Bragg scattering). The existence of an apparently stable phase amorphous on such a long length scale is very interesting. There is much speculation on the existence of ideal glassy state,[24] which is approached asymptotically as one quenches arbitrarily slowly. The fact that, in certain parameter ranges, cholesteric fluids appear to have an amorphous ground state may have relevance to these ideas. (Note that the fog seems to be the most elusive of the blue phases.)

Sachdev and Nelson[31] have understood properties of the metallic glasses as Gaussian fluctuations about the isotropic state. Although Hornreich and Shtrikman[32] claim that fluctuations in the isotropic state cannot explain the blue fog, it is possible that they are wrong. Clearly, one must perform the analogous calculation for the blue phase. It would be fascinating if the blue fog were a precise analog of the metallic glasses.

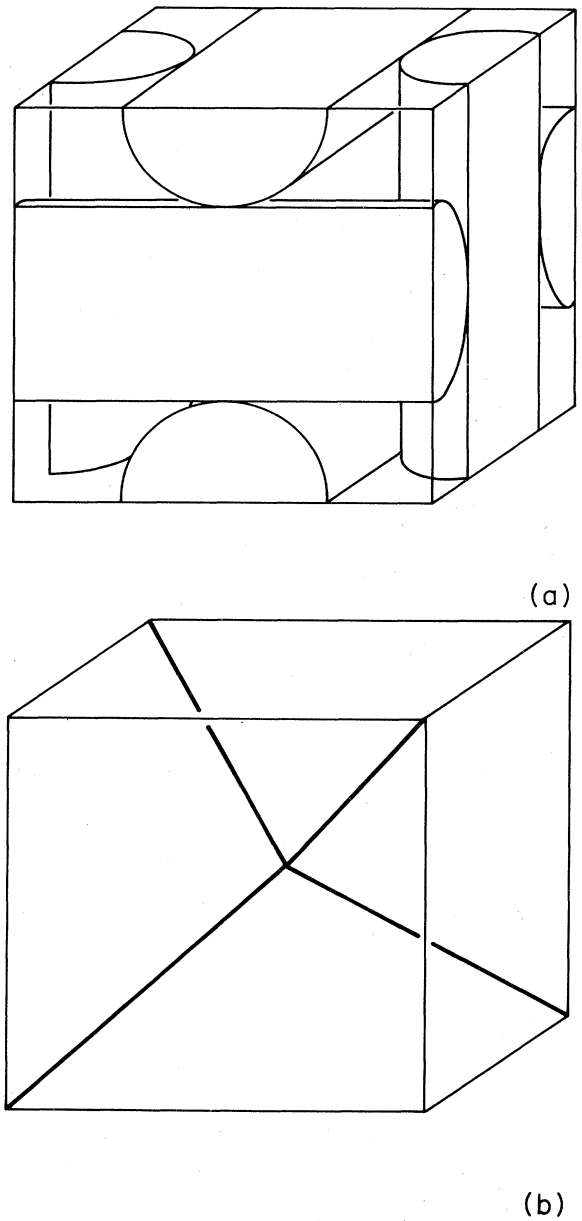

FIG. 14. (a) *Crystalline blue phase: tube structure.* Proposed model for blue phase II, shown as an array of 45° tubes. (b) *Defect structure.* The same model blue phase, showing the $s=-\frac{1}{2}$ defect lines in the unit cell.

We can form a model blue phase out of the 45° tubes in Fig. 12, which is consistent with the present experimental data on blue phase II.[1] (Most, although not all, of the proposed model blue phases can be interpreted in terms of double-twist tubes. The defect-line description can be used in all models, because it is topological.) One can pack these tubes into a cubic array [Fig. 14(a)], defining the "O^2" phase.[2] Defect lines pass through the right-handed corners, and meet in the center of the unit cell [Fig. 14(b)]. Each corner of the unit cell has also four defect lines passing from it; the defect lines form two interpenetrating diamond lattices.

III. IDEAL TEMPLATES

In the preceding section we saw that cholesteric fluids and metallic glasses are frustrated: the local low-energy structures cannot be used to fill space. In this section, we shall begin by seeing that both of these systems are unfrustrated in an unphysical space—the surface S^3 of a sphere in four dimensions. We shall refer to these ideal, unfrustrated configurations as "templates" for the real flat-space structures. The defect lines will have a natural interpretation as the edges of the cuts needed to flatten the spherical templates.

In Fig. 4, we saw that when five undistorted tetrahedra are fit around an edge, there is a $7\frac{1}{2}°$ gap. If we go to a space of positive curvature, we can shorten the circumference of a circle while keeping its radius fixed; in particular, on the surface of a sphere of radius $\kappa^{-1}\simeq 1.59a$, five tetrahedra of edge length a will join together perfectly at an edge. This process can be continued to form a Euclidean solid in four dimensions. 600 tetrahedra will smoothly cover S^3 with five tetrahedra meeting at each edge. This solid has 120 vertices, so 120 atoms of diameter a can be fit onto a sphere of radius κ^{-1}; the neighbors of each atom form an icosahedron. This ideal template was described long ago by Coxeter[16] (it is polytope $\{3,3,5\}$). It was proposed as a model for metallic glasses by Sadoc[14] and Kléman,[15] and has been studied in detail by Nelson.[6]

Cholesteric fluid can have double twist everywhere on the surface of a sphere of radius q^{-1}. If $x=(x_0,x_1,x_2,x_3)$ is a point on the sphere, then the ideal template is given by the vector field

$$n(x)=q(-x_1,x_0,x_3,-x_2)\ . \tag{3.1}$$

This is a unit-vector field ($n^2=1$) everywhere tangent to the sphere ($n\cdot x=0$). Most important, it has double twist everywhere,[12,1] $n_{i;j}=-q\epsilon_{ijk}n_k$.[33] We now check explicitly that it has double twist in the neighborhood of the top of the sphere. At $x_0=(q^{-1},\epsilon_x,\epsilon_y,\epsilon_z)$,

$$n(x_0)=(-q\epsilon_x,1,q\epsilon_z,-q\epsilon_y)\ . \tag{3.2}$$

The first component represents the change in $\mathbf{n}$ necessary for it to remain tangent to the sphere [$\mathbf{n}(x_0)$ points in the

$\hat{x}$ direction; since x_0 is at the top of the sphere, moving a distance ϵ_x in the $\hat{x}$ direction must shift $\mathbf{n}$ downward]. The last two represent a right-handed double twist of pitch $2\pi/q$; if I advance in the $\hat{z}$ direction $\mathbf{n}$ twists in the $+\hat{y}$ direction, if I advance in the $\hat{y}$ direction $\mathbf{n}$ twists in the $-\hat{z}$ direction. The blue-phase template was proposed first in a conversation between Doug Eardley and Nelson; Nelson then communicated it to us.[17,34,35] Notice that the circumference of the sphere equals the pitch of the cholesteric, so for example along the circle $x_1=x_2=0$, $n(x)$ rotates by 2π. Along the circles $x_2=x_3=0$ and $x_0=x_1=0$, $n(x)$ always is tangent to the circle; one can think of the template 3.1 as two 45° double-twist tubes centered at these circles and glued along the surface $x_0^2+x_1^2=x_2^2+x_3^2=\frac{1}{2}$.[36] [This decomposition is not unique; any left-handed rotation will give another separation of (3.1) into tubes.]

The defect lines now have a geometrical interpretation: They are the disclination lines which form the edges of the cuts needed to flatten the sphere. Consider the problem in one lower dimension—making a carpet out of orange peel. To flatten a piece of peel, one can ease the strains by cutting into the center of the piece. One must naturally fill in the empty wedge with more peel (Fig. 15). This can be done so as to leave no seam; however, the vertex of the wedge remains a point of high strain energy, and the resulting carpet will be a lattice of interacting point disclinations. In the same way, the line disclinations in our frustrated theories are the edges of cuts in the ideal templates on S^3. In our problems of course the size of the wedge of material we may add is restricted. For cholesteric fluids we must add a full half-plane of fluid in order to keep the molecular orientations smooth at the boundaries (the "seams"); the defect formed is the $s=-\frac{1}{2}$ line (Fig. 13). For metallic glasses we must add whole tetrahedra (if we cut at an edge).

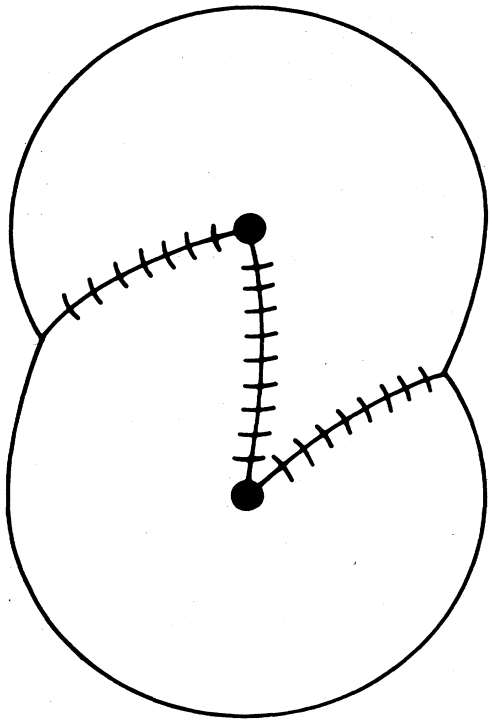

FIG. 15. *Orange-peel carpet.*

Cholesteric fluids are continuous on the length scales of the pitch $2\pi/q$ since the molecular size is much smaller than the radius of the unfrustrated spherical template. Notice that this is not true of the metallic glasses—there the atomic spacing a is not small compared to the radius $\kappa^{-1}=1.59a$. Thus there is no natural separation between the physics of the individual atoms and the physics of flattening the spherical template. This is represented, for example, by the fact that 40—60% of the atoms occupy defect sites.[6] One may question the utility of an ideal template which describes the local ordering to at most one or two atomic lengths. We hope that the complexities introduced by the large lattice cutoff are uninteresting, and the important physics is retained as one takes a continuum limit. Keep in mind that the continuum theory for metallic glasses we develop in the next sections is an uncontrolled approximation. In principle, details about the interparticle forces can be important. (This problem is shared by the Landau theories of metallic glasses.[13,31]) In Sec. VI we shall show that any properties which are preserved in the continuum limit are universal. One can only hope that the universal, model-independent properties explain interesting physical effects.

IV. TOPOLOGICAL ORDER PARAMETERS[37]

Choosing an order parameter appears to be something of an art. Two systematic methods have been used in the blue-phase and metallic glass problems. Which method is more accurate depends upon the importance of fluctuations—how strongly first order the transition is.

For second-order and weakly-first-order transitions, one can make a Landau expansion of the free energy. In the blue phase, the Landau expansion was introduced by Brazovskii and Dmitriev,[11] and has been pursued in detail by Hornreich and Shtrikman[12] and Wright and Mermin.[1,17] Consider the distribution of molecular orientations found in a small volume of cholesteric fluid surrounding a point $\mathbf{r}$. (The volume must be small compared to the pitch.) The orientations can be thought of as points on the surface of a sphere. In the isotropic phase, this distribution is spherically symmetric: The orientational correlations have only short-range order. If the isotropic phase undergoes a weakly-first-order phase transition, the deviation from spherical symmetry will be small. Usually it is assumed that the first nonzero multipole moment of the distribution will be large compared to the succeeding moments. The effects of the higher-order moments are absorbed into effective elastic constants. In the broken-symmetry phases of the cholesteric fluids, the dipole moment vanishes. (This is why the ends of the molecules are assumed to be indistinguishable.) Thus the quadrupole moment—a symmetric traceless tensor $Q_{\alpha\beta}(\mathbf{r})$—forms the order parameter. The free energy is then written as a power series in Q and gradients of Q. Landau theory provides a "soft-spin" order parameter, and a free energy which is asymptotically valid as the transition approaches

second order. Defect lines, however, lose their meaning in this description. When we associate a director $\vec{n}$ to the major axis of the quadrupole moment (i.e., the direction of largest probability: the eigenvector of Q with largest eigenvalue), the core of the topological defect line in n can relax by going biaxial. At the center of the core, the order parameter Q develops two degenerate axes of maximum probability.

[The blue phases are probably not stable for strongly-first-order phase transitions. Within Landau theory they are stable in the "high chirality" limit[12] when the correlation length is large compared to the pitch. Within a director description the core size of the disclination lines must be comparable to the pitch;[2] the correlation length must be comparable to the core size to keep the surface tension energy small[38] (see Sec. VI). However, Sec. VI will provide a renormalization-group justification for taking the correlation length to zero, allowing us to study defect lines with a director order parameter.]

The Landau theory for metallic glasses is much more complicated. Steinhardt *et al.*[39] introduced a 13-component order parameter intended to describe the local icosahedral orientational order; it transformed under the spin-six representation of SO(3) (the blue-phase quadrupolar order parameter is spin two). This proved unsatisfactory, as it is not possible to write a frustrated free energy of the required form using only orientational order[10] (e.g., without including translational order). Based partially on the ideas presented in the next section, Nelson and Widom[13] have constructed a 169-component order parameter describing both the local orientational order and the local translational order; it transforms under the smallest representation of SO(4) broken by the symmetry of the ideal template. If the analogies with the blue phase continue to hold, many interesting results can be expected. In particular, one should be able to study systematically the stability of the Frank-Kasper phases within Landau theory. I will not pursue Landau theory in this paper.

For strongly-first-order phase transitions, fluctuations in the magnitude of the order parameter are not as important, and cannot be treated systematically. In the broken-symmetry phase there are many degenerate ground states. It is appropriate to characterize the state of the material at a point $\mathbf{r}$ by the ground state most closely approximating the local environment of $\mathbf{r}$. The order parameter labels the different ground states ("degenerate vacuum states" in field theory). I call this a topological order parameter (as opposed to a Landau order parameter) because it was used in the topological classification of defects.[40] Naturally, when the local environment of $\mathbf{r}$ is strained it is not perfectly described by any ground state. However, if the gradients are small, the additional strain degrees of freedom should be slaves to the order-parameter field, and can be absorbed into effective elastic constants. Before defining the metallic glass and blue-phase order parameters, I will give two examples to establish my conventions.

We start with translational order in a one-dimensional crystal with four atoms per unit cell (Figs. 16). The order parameter at a point r must represent the broken translational symmetry; it should determine the position of r within its local unit cell. For example, in Fig. 16(a), the

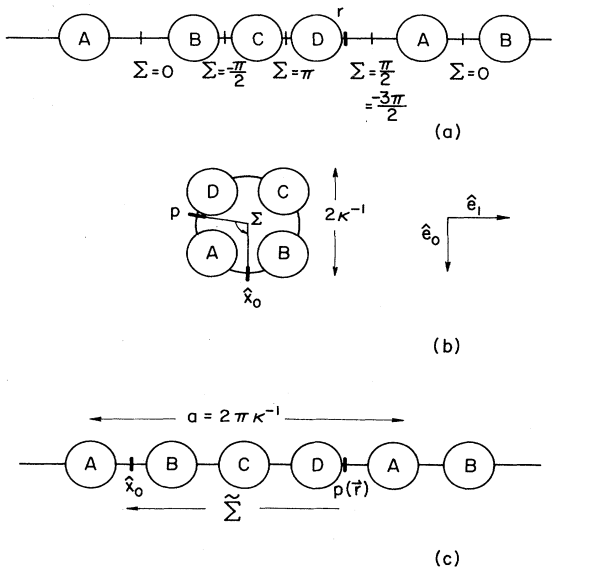

FIG. 16. *One-dimensional crystal with four atoms per unit cell.* (a) Real configuration of strained crystal. (b) Circular order parameter space describing translational order within the unit cell. $\hat{x}_0$ is an arbitrarily distinguished reference point. (c) Ideal periodic crystalline template: undistorted crystal.

order parameter at r must indicate that r lies close to atom D, between it and A.

There are two natural templates in this problem [Figs. 16(b) and 16(c)]; both give equivalent order parameters and both have natural analogs in the more complicated problem. In both the circular template and the periodic crystalline template, one can locate a point $p(r)$ giving the location of r within its unit cell. Thus $p(r)$ maps the distorted structure into the ideal template. We could use p as an order parameter. However, it is the operation Σ (roughly translation by $-p$) which will generalize properly to an order parameter in the more complicated systems. To define Σ for the circular template [Fig. 16(b)], we choose a distinguished point $\hat{x}_0=(\kappa^{-1},0)$ on the circle. (Think of the circle as lying tangent at $\hat{x}_0$ to physical space at r.) Then if $p=(p_0,p_1)$ is the point on the template corresponding to r,

$$\Sigma=\begin{bmatrix} \kappa p_0 & \kappa p_1 \\ -\kappa p_1 & \kappa p_0 \end{bmatrix}$$

is that rotation of the circle [element of SO(2)] which takes p to $\hat{x}_0$. For the periodic crystalline template [Fig. 16(c)], we first define $\tilde{\Sigma}$ to be the translation taking p to $\hat{x}_0$. However, since the ideal ground state is invariant under translation by a lattice constant $a=2\pi\kappa^{-1}$, translations $\tilde{\Sigma}_1$ and $\tilde{\Sigma}_2$ are equivalent if they differ by $2\pi n\kappa^{-1}$ [$\tilde{\Sigma}_1^{-1}\tilde{\Sigma}_2(x)=x-na$]. The order parameter Σ is thus an equivalence class of translations $\{\tilde{\Sigma}g\colon\ g(x)=x-na\}$. These two constructions give equivalent order parameters: rotations by θ correspond to translations by $\kappa^{-1}\theta$.

Now we find the topological order parameter for a

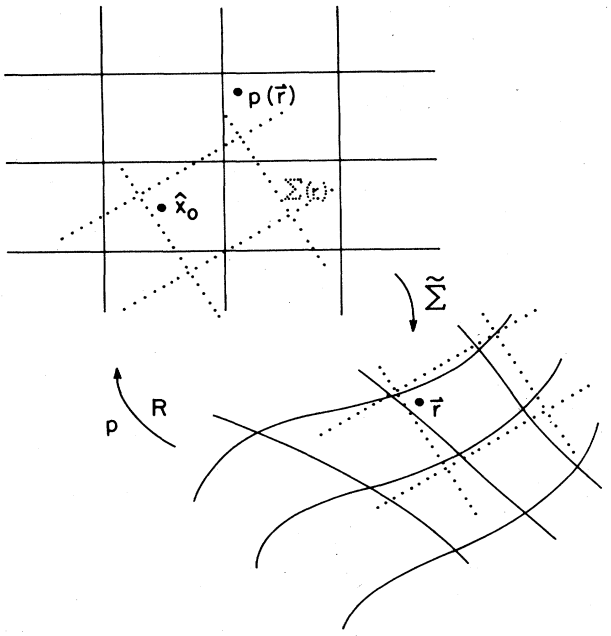

FIG. 17. *Two-dimensional crystal.* To align the distorted physical crystal at **r** with the ideal template, one rotates by R and the translates by p. To align the ideal template to physical space, one applies the Euclidean transformation $\tilde{\Sigma}=(-p,R^{-1})$.

crystal lattice with dimension greater than one (Fig. 17). We again want to describe the configuration in the neighborhood of a point r by matching it as closely as possible to a region on the ideal template. Here there is a larger class of degenerate ground states since rotations as well as translations of the ideal template will have zero energy. Thus the order parameter at a point r must determine both a point $p(r)$ on the ideal template giving the position within the unit cell and a rotation $R(r)$ needed to align the unit cell containing r to the axes of the ideal structure. R and p define a unique Euclidean transformation $\tilde{\Sigma}=(-p,R^{-1})$ which shifts p to the origin $\hat{x}_0$ and aligns the ideal template to the unit cell containing r, so that $\tilde{\Sigma}(x)=R^{-1}(x-p)$ (Fig. 17). The template has a symmetry group G_c, which in Fig. 17 consists of lattice translations and rotations by 180°. Two Euclidean transformations $\tilde{\Sigma}_1$, $\tilde{\Sigma}_2$ are equivalent if $\tilde{\Sigma}_1^{-1}\tilde{\Sigma}_2 \in G_c$. If $\tilde{\Sigma}_1^{-1}\tilde{\Sigma}_2 \in G_c$ then either $R_1=R_2$ and p_1-p_2 is a lattice vector (so p_1 and p_2 are in the same place within the unit cell) or $R_1=-R_2$ and p_1+p_2 is a lattice vector (p_2 and $-p_2$ are in equivalent places because of the 180° rotation symmetry). The order-parameter space is the right coset space $E(2)/G_c$ formed by these equivalence classes.

Notice that this order parameter is not completely satisfactory since R and p are not independent in the physical system. The configuration of the distorted crystal in Fig. 17 is fully specified by the translation field $p(r)$; $p^{-1}(x)$ maps the ideal template onto the distorted structure and thus determines precisely the distortion. The rotation field $R(r)$ is determined by the gradients of $p(r)$ in any order parameter field which is physically realizable, since if I know the location of the points near r in the unit cell, I can determine the orientation. We shall see in the next section that there is a unique decomposition

$$\partial_j p_i=(\delta_{ik}-e_{ik})R_{kj}\ , \tag{4.1}$$

where e_{ik} is the (symmetric) strain matrix. The rotation R_{ij} represents extra degrees of freedom in the order-parameter field which are not present in the original material. Such extra degrees of freedom occur whenever translation invariance is broken. They cause serious problems, for example, in the topological classification of defects.[40] We shall see in the next section that the free energy constrains the R_{ij} to satisfy (4.1) in static equilibrium. The new degrees of freedom are high-frequency modes (have a "mass") and should not change the long-wavelength properties of the theory. However, an ideal theory would not include these extra modes.

Using these analogies, the metallic glass (MG) order parameter is easy to construct. The ideal template lies on the surface of a sphere S^3 in four dimensions. The symmetries of the sphere form the rotation group SO(4). The template breaks this symmetry; the symmetry group $G_{\rm MG}$ of the template is a discrete set of 7200 rotations (described in detail by Nelson and Widom[13]). The order parameter at a point **r** in physical space will represent the broken rotational symmetry of the curved template.

This broken rotational symmetry will combine translational and orientational information about the neighborhood of **r**. The point **r** lies in a certain position within its local tetrahedron (or pentagon, in Fig. 18). The order parameter must determine a point $p(\mathbf{r})$ at a corresponding position within a unit cell on the ideal template. It must also determine a rotation $R(\mathbf{r})$, which will align the two unit cells. Let Latin indices run from 1 to 3 and Greek indices run from 0 to 3. The p_μ is a point on the sphere ($p_\mu p_\mu=\kappa^{-2}$), and contains translational information. R_{vj} is a 4×3 matrix which orients the physical tetrahedron at **r** tangent to the ideal tetrahedron at p.

To make things precise, we must specify an initial orientation of the template. (The arbitrary choice of this initial orientation will lead to a local gauge invariance in Appendix B.) Choose the point $\hat{x}_0=(\kappa^{-1},0,0,0)$ to be the point on S^3 "tangent" to R^3 at **r**. [That is, the point $\hat{x}_0$ is identified with r, and the point $(0,\epsilon_x,\epsilon_y,\epsilon_z)$ in the tangent space at $\hat{x}_0$ is identified with the point $(\epsilon_x,\epsilon_y,\epsilon_z)$

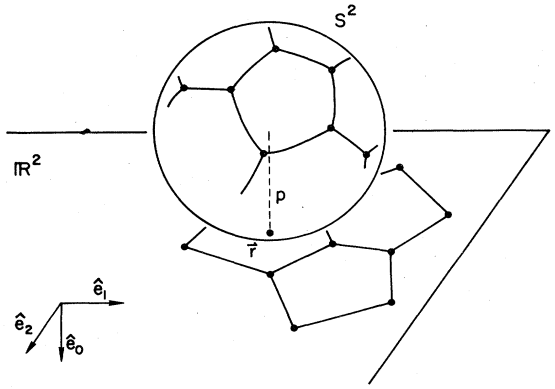

FIG. 18. *Covariant derivative is given by rolling the sphere.* The ideal structure on the spherical template projects onto the local low-energy structure in physical space.

in the tangent space at r.] The rotation Σ will take p to $\hat{x}_0$ and align the local tetrahedron around p with the distorted tetrahedron in flat space tangent to $\hat{x}_0$.

We can write the components $\tilde{\Sigma}_{\mu\nu}$ in terms of p_μ and $R_{\nu j}$. $\tilde{\Sigma}$ takes p_ν to $\hat{x}_0=\kappa^{-1}\delta_{0\mu}$, so that

$$p_\nu=(\tilde{\Sigma}^{-1})_{\nu\mu}\hat{x}_\mu=(\tilde{\Sigma}^{T})_{\nu\mu}\hat{x}_\mu=\tilde{\Sigma}_{\mu\nu}\hat{x}_\mu=\kappa^{-1}\tilde{\Sigma}_{0\nu}\ . \quad (4.2)$$

The rotation R maps the real tetrahedron onto the ideal tetrahedron; $\tilde{\Sigma}$ then maps the ideal one onto the real one, so $\tilde{\Sigma}_{\mu\nu}R_{\nu j}=\delta_{\mu j}$,

$$R_{\nu j}=(\tilde{\Sigma}^{-1})_{\nu\mu}\delta_{\mu j}=\tilde{\Sigma}_{j\nu}\ , \quad (4.3)$$

$$\tilde{\Sigma}=\begin{bmatrix}\kappa^{-1}p_0 & \kappa^{-1}p_1 & \kappa^{-1}p_2 & \kappa^{-1}p_3\\ R_{01} & R_{11} & R_{21} & R_{31}\\ R_{02} & R_{12} & R_{22} & R_{32}\\ R_{03} & R_{13} & R_{23} & R_{33}\end{bmatrix}\ . \quad (4.4)$$

Thus p and R explicitly determine $\tilde{\Sigma}$.

If $\mathbf{r}$ is in a corner of a tetrahedron, then $p(\hat{\mathbf{r}})$ can be in any corner of any of the 600 tetrahedra in the template. The order parameter is only defined up to a symmetry operation of the ideal template. If I rotate by any of the symmetries $g\in G_{\rm MG}$ before I rotate by $\tilde{\Sigma}(\mathbf{r})$, it defines a new rotation $\tilde{\Sigma}'$ which corresponds to the same physical environment of $\mathbf{r}$. The order parameter $\Sigma(\mathbf{r})$ is an equivalence class,

$$\Sigma(r)=\{\tilde{\Sigma}'\colon \tilde{\Sigma}'=\tilde{\Sigma}(r)g, g\in G_{\rm MG}\}\ , \quad (4.5)$$

and the order-parameter space is the right coset space $SO(4)/G_{\rm MG}$.

We will continue to treat the metallic glass order parameter as an SO(4) rotation. The quotient structure of the order parameter is important in classifying the allowed defect lines.[37,13,6] However, since the symmetry group of the metallic glass template $G_{\rm MG}$ is discrete, the equivalence classes do not change the local differential structure of the order parameter. In this paper we study the energetics of the mildly strained regions between defect lines, where these discrete equivalences are unimportant complications.

Unlike the metallic glasses, the symmetry group $G_{\rm BP}$ of the blue-phase (BP) template,

$$n(\mathbf{x})=q(-x_1,x_0,x_3,-x_2)\ , \quad (4.6)$$

is a continuous group, and the equivalence classes do change the form of the order parameter. Just as in the metallic glass, the order-parameter space is $SO(4)/G_{\rm BP}$. In the metallic glasses, the symmetry group is discrete (zero dimensional) and the order parameter has six independent components, since SO(4) is a six-dimensional space. We will see here that $G_{\rm BP}$ is a four-dimensional group, and the topological order parameter for the cholesteric fluid will have two independent components. Indeed, the blue-phase order parameter will be a director (a headless vector).

An infinitesimal rotation $\tilde{\Sigma}_\epsilon=\delta_{\alpha\beta}+\epsilon J_{\alpha\beta}$ in SO(4) is a symmetry of the template $n(\mathbf{x})$ if

$$\begin{aligned}n_\alpha(\mathbf{x})&=\tilde{\Sigma}_{\alpha\beta}n_\beta((\tilde{\Sigma}^{-1})_{\rho\sigma}x_\sigma)\\ &=(\delta_{\alpha\beta}+\epsilon J_{\alpha\beta})n_\beta((\delta_{\rho\sigma}-\epsilon J_{\rho\sigma})x_\sigma)\\ &=n_\alpha(\mathbf{x})+\epsilon[J_{\alpha\beta}n_\beta-(\partial_\rho n_\alpha)J_{\rho\sigma}x_\sigma]\ .\end{aligned} \quad (4.7)$$

Since $n(\mathbf{x})$ is linear in $\mathbf{x}$, $(\partial_\sigma n_\beta)x_\sigma=n_\beta$. Therefore J preserves n if $(J_{\alpha\beta}\partial_\sigma n_\beta-\partial_\rho n_\alpha J_{\rho\sigma})x_\sigma=0$. Since this must be true for all x, and $J_{\alpha\beta}=-J_{\beta\alpha}$, J preserves n if

$$[J,\partial n]=J_{\sigma\rho}\partial_\rho n_\alpha-\partial_\sigma n_\beta J_{\beta\alpha}=0\ . \quad (4.8)$$

There is a four-dimensional set of solutions to (4.8):

$$J_{ij}=\begin{bmatrix}0 & A & C & D\\ -A & 0 & D & -C\\ -C & -D & 0 & B\\ -D & C & -B & 0\end{bmatrix}\ ; \quad (4.9)$$

these form a Lie subalgebra $g_{\rm BP}$ in the Lie algebra so(4) of infinitesimal rotations.

Consider the action of the infinitesimal rotations (4.9) near $\hat{x}_0=(\kappa^{-1},0,0,0)$. B generates rotations which leave $\hat{x}_0$ and $n(\hat{x}_0)$ fixed—rotating about $n(\hat{x}_0)=(0,1,0,0)$; A, C, and D move $\hat{x}_0$ to other points on S^3. The Lie algebra quotient $so(4)/g_{\rm BP}$ is spanned by the rotations leaving $\hat{x}_0$ fixed but changing $n(\hat{x}_0)$:

$$J_{ij}=\begin{bmatrix}0 & 0 & Q & 0\\ 0 & 0 & P & 0\\ -Q & -P & 0 & 0\\ 0 & 0 & 0 & 0\end{bmatrix}\ . \quad (4.10)$$

This implies that two rotations are equivalent if they leave $n(\hat{x}_0)$ pointing in the same direction. More precisely, $\tilde{\Sigma}_1$ and $\tilde{\Sigma}_2$ are equivalent if $\tilde{\Sigma}_1 n(\tilde{\Sigma}_1^{-1}\hat{x}_0)=\tilde{\Sigma}_2 n(\tilde{\Sigma}_2^{-1}\hat{x}_0)$. Thus the equivalence classes of rotations can be labeled by the unit vector $n(\mathbf{r})=\Sigma n(\Sigma^{-1}\hat{x}_0)$. Finally, we must include the discrete symmetry of the template (4.6); since the ends of the molecules are not distinguished, $n(\mathbf{x})$ and $-n(\mathbf{x})$ describe the same template. $G_{\rm BP}$ contains this discrete symmetry, and the rotations in $SO(4)/G_{\rm BP}$ labeled by $n(\hat{x}_0)$ and $-n(\hat{x}_0)$ are equivalent.

Thus the order parameter Σ for the metallic glasses is an SO(4) rotation (modulo equivalences), which describes the translational order within the unit cell together with the orientational order of the unit cell. The blue-phase order parameter n is a director.[41]

V. COVARIANT DERIVATIES AND FREE ENERGIES

In this section we shall use the ideal templates and the order parameters of the previous two sections to construct covariant derivatives and continuum elastic energies. We will develop first the elastic theory of (flat space) crystals and second the theory of the blue phase. Both are already well understood (although our treatment is unorthodox). However, each will illuminate important features of the theory of metallic glasses, with which we conclude this section.

Usually, the order parameter field in the ideal ground state is constant (e.g., in ferromagnets) and the elastic energy is quadratic in the gradients of the order parameter.

In our materials, the order parameter varies with position. In the blue phases, the order parameter has a "double twist" [Eq. (2.2)]. In crystals and the metallic glasses, the translational components of the order parameter [$p(r)$ in Eq. (4.2)] vary as one moves across the local unit cell. We will construct covariant derivatives which are zero for the order parameter variation characteristic of the ideal state. We will then make free energies quadratic in these covariant derivatives. This provides a natural method for calculating elastic energies of small deformations from the ideal state.[42]

The elastic theory of (flat-space) crystals is unfrustrated. However, it does treat both orientational and translational order—which are necessary features of the theory of metallic glasses. Traditional continuum elastic theory[43] describes the deformation of the crystal of a displacement field $u(\mathbf{x})$. In the notation of the preceding section (Fig. 17) $u(\mathbf{x})=p^{-1}(\mathbf{x})-\mathbf{x}$. [$p^{-1}(\mathbf{x})$ is the position in the distorted crystal corresponding to $\mathbf{x}$.] Although $u(\mathbf{x})$ can be large (e.g., in a uniform compression), the gradients $\partial_i u_j$ in the naive theory are assumed small. The elastic energy can then only depend on the symmetric strain $e_{ij}=(\partial_i u_j+\partial_j u_i)/2$; the antisymmetric part corresponds to an infinitesimal local rotation, which cannot change the energy. The most general free-energy density for a homogeneous, isotropic medium is then

$$F=2\mu(e_{ij})^2+\lambda(e_{ii})^2 . \tag{5.1}$$

The naive form of the theory involves an unnecessary assumption, and is not sufficient for our purposes. We need to study disclination lines (Fig. 19). Far from a disclination, the crystal is not strained much; however, it is in general rotated by a finite rotation $p(\mathbf{r})\simeq R\mathbf{r}$, and $\partial_i u_j=R_{ji}-\delta_{ij}$ is not small. In particular, a simple rotation by an angle θ in this theory costs an energy $4(\mu+\lambda)(\cos\theta-1)^2$. Traditional, naive elastic theory fails for large rotations.

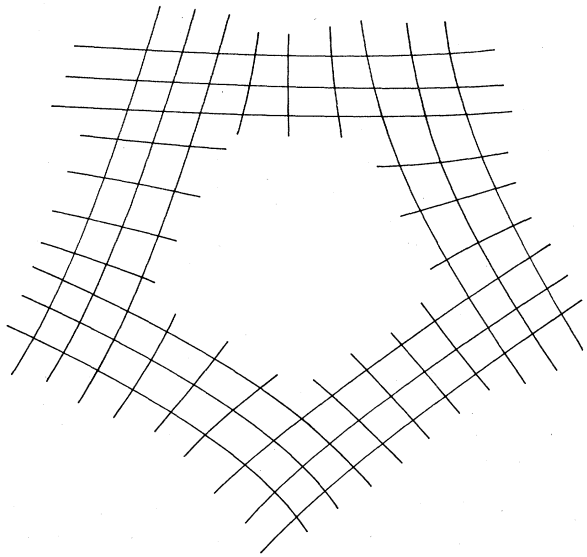

FIG. 19. *Disclination lines have large rotations.* The strains far from a disclination line are small, but even in the far field the crystal is rotated a finite angle.

This problem can be cured by a more careful definition of the strain matrix. Landau and Lifshitz[44] add an extra term to e_{ij}:

$$e_{ij}=\frac{1}{2}\left[\partial_i u_j+\partial_j u_i+\frac{\partial u_k}{\partial x_i}\frac{\partial u_k}{\partial x_j}\right]$$

$$=\tfrac{1}{2}(\partial_i p_k^{-1}\partial_j p_k^{-1}-\delta_{ij}) . \tag{5.2}$$

This new strain matrix is rotation invariant; if a deformation p^{-1} is followed by a rotation R, then since $R^T=R^{-1}$,

$$\partial_i(Rp^{-1})_k\partial_j(Rp^{-1})_k-\delta_{ij}=(R_{km}\partial_i p_m^{-1})(R_{kn}\partial_j p_n^{-1})-\delta_{ij}$$

$$=\partial_i p_k^{-1}\partial_j p_k^{-1}-\delta_{ij}=e_{ij} . \tag{5.3}$$

Although this is undoubtably the simplest cure for the problem, it is not the only one. Any matrix can be uniquely decomposed into a symmetric matrix times a rotation (the polar decomposition). Let us decompose ∂p into (4.1):

$$\partial_j p_i=(\delta_{ik}-e_{ik})R_{kj} . \tag{5.4}$$

A point $\mathbf{r}+\boldsymbol{\xi}$ near $\mathbf{r}$ is a strained image of a point $\mathbf{p}+\boldsymbol{\pi}$ near $\mathbf{p}$, where $\pi_j=\xi_i\partial_i p_j$. Equation (5.4) insures that to first order in e the ideal template is strained by e and then rotated by R^{-1}:

$$\xi_i=\pi_j\partial_j p_i^{-1}=R_{ki}(\delta_{kj}+e_{kj})\pi_j+O(e^2) . \tag{5.5}$$

We can define the strain matrix using (5.4) to be

$$e_{ij}=\delta_{ij}-R_{ik}\partial_k p_j , \tag{5.6}$$

where R is chosen to make e symmetric and is in some sense the rotation closest to $\partial_i p_j$. Using Eq. (5.5), it is easy to see that (5.2) and (5.6) are equal to lowest order in e, and are equivalent within linear elastic theory.

The strain matrix is a covariant derivative, since it is zero in the undeformed (but rotated) crystal and it expresses the deviation from the undeformed state. In the preceding section, we defined the order-parameter space for a crystalline lattice to be the Euclidean transformations $(-p,R^{-1})$. Equation (5.5) provides us with a covariant derivative on this space, and (5.1) gives us the free energy (if we ignore crystalline anisotropy):

$$F=2\mu(\delta_{ij}-R_{ik}\partial_k p_j)^2+\lambda(3-R_{ik}\partial_k p_i)^2 . \tag{5.7}$$

The strain matrix determined by this decomposition is symmetric. As noted in the preceding section, we have introduced new degrees of freedom by allowing R to vary independently of the gradients of p; in principle these allow e to become asymmetric. We can show, however, that in regions of small strain, small deviations of R from its decomposition value will always increase the energy. Let p and $\bar{R}$ define the order-parameter field, with covariant derivative $\bar{e}$ [Eq. (5.6)]. Let R be defined by the singular value decomposition of ∂p, and e be the (symmetric) strain field. Assume R and $\bar{R}$ are nearly the same: $\bar{R}_{ik}=R_{lk}(\delta_{li}+\epsilon_{li})$. Then

$$\bar{e}_{ij}=\delta_{ij}-(\delta_{li}+\epsilon_{li})R_{lk}\partial_k p_j$$
$$=e_{ij}+\epsilon_{ij}-\epsilon_{il}e_{lj}=e_{ij}+\epsilon_{ij}+O(e\epsilon)\ ,$$

and the change in the energy (5.1) is $2\mu(\epsilon_{ij})^2>0$. (However, if $\lambda\gg\mu$, large rotations can lower the energy.[45]) Thus the free energy provides a uniform restoring force which resists deviations of these extra modes from their proper values.

It would be natural now to construct the covariant derivative for the blue phase from the ideal double-twist template [Eq. (3.1)]:

$$n^I(x)=q(-x_1,x_0,x_3,-x_2)\ . \tag{5.8}$$

This is a formal exercise, since the covariant derivative will of course be the deviation from the ideal double-twist state of Eq. (2.2):

$$(D_i n)_j=\partial_i n_j+q\epsilon_{ijk}n_k\ . \tag{5.9}$$

This construction is precisely analogous to the metallic glass covariant derivative construction that follows. However, things are complicated by the quotient structure of the order-parameter space. We will confine this illuminating but distracting calculation to Appendix A.

The elastic theory for the blue phase has been pursued in some detail.[1-3,10-12,17] If we sum the squares of the components of our covariant derivative (5.9), we get the Frank free-energy density in the "one-constant approximation," plus a total divergence:

$$F\{n\}=\tfrac{1}{2}K(D_i n)_j(D_i n)_j$$
$$=\tfrac{1}{2}K\{(\mathrm{div}n)^2+(n\times\mathrm{curl}n)^2+(n\cdot\mathrm{curl}n+q)^2$$
$$+\mathrm{div}[n\cdot\nabla n-n\nabla\cdot n]+q^2\}\ . \tag{5.10}$$

In the most general Frank free energy, each of the four terms in (5.10) can have an independent elastic constant. By using other scalars formed from n and Dn, Wright has expressed the general free energy in terms of covariant derivatives.[46]

The total divergence term in (5.10) *cannot* be dropped, even though it is a surface energy.[2] In the blue phase there is a finite density of disclination lines. To integrate by parts, one must exclude the core of each defect line. The boundaries of these cores give the blue phase a finite "internal surface area" per unit volume. We will see in the next section that the flux of $n\cdot\nabla n-n\nabla\cdot n$ through these surfaces acts as a measure of the length of the disclination lines.

We now come to the central result of this paper, the continuum theory for the metallic glasses. The local state at a point $\mathbf{r}$ in a metallic glass is given by a rotation $\Sigma(\mathbf{r})$ of the ideal template. $\Sigma(\mathbf{r})$ rotates the template to change the orientation and position of one of its tetrahedra, aligning it with the tetrahedron of metal atoms in physical space surrounding $\mathbf{r}$. The covariant derivative, recall, is a rule telling how the system varies from point to point to minimize the energy. We will define the covariant derivative by rolling the sphere along physical space without slipping[15] (Fig. 18). To roll the sphere a small distance $\boldsymbol{\xi}=\xi_1\hat{\mathbf{e}}_1+\xi_2\hat{\mathbf{e}}_2+\xi_3\hat{\mathbf{e}}_3$, one uses the rotation

$$\Sigma_{\boldsymbol{\xi}}=\exp(\kappa\xi_i J_i)\simeq\mathbb{1}+\kappa\xi_i J_i\ , \tag{5.11}$$

where

$$(J_i)_{\mu\nu}=\delta_{0\mu}\delta_{i\nu}-\delta_{i\mu}\delta_{0\nu}\ . \tag{5.12}$$

To form the ideal low energy state near $\mathbf{r}$ we first align the template to $\mathbf{r}$ using $\Sigma(\mathbf{r})$ and then roll it to $\mathbf{r}+\boldsymbol{\xi}$. This defines a parallel transported (PT) rotation field Σ^{PT}:

$$\Sigma^{\mathrm{PT}}(\mathbf{r}+\boldsymbol{\xi})=\Sigma_{\boldsymbol{\xi}}\Sigma(\mathbf{r})\ . \tag{5.13}$$

The covariant derivative thus measures the deviation of $\Sigma(\mathbf{r}+\boldsymbol{\xi})$ from $\Sigma_{\boldsymbol{\xi}}\Sigma(\mathbf{r})$.

We define the covariant derivative $D\Sigma$ to be

$$(D_i\Sigma)_{\mu\nu}=\lim_{\xi\to 0}\left[\frac{\Sigma(\mathbf{r}+\xi\hat{\mathbf{e}}_i)[\Sigma_{\xi\hat{\mathbf{e}}_i}\Sigma(\mathbf{r})]^{-1}-\mathbb{1}}{\xi}\right]$$
$$=(\partial_i\Sigma_{\mu\rho})\Sigma^{-1}_{\rho\nu}-\kappa J_{i\mu\nu}=(\partial_i\Sigma_{\mu\rho})\Sigma_{\nu\rho}-\kappa J_{i\mu\nu}\ . \tag{5.14}$$

This definition ensures that $D\Sigma$ is antisymmetric in μ and ν [since

$$(\partial_i\Sigma_{\mu\rho})\Sigma_{\nu\rho}+(\partial_i\Sigma_{\nu\rho})\Sigma_{\mu\rho}=\partial_i(\Sigma_{\mu\rho}\Sigma_{\nu\rho})=\partial_i(\delta_{\mu\nu})=0$$

and $J_{i\mu\nu}=-J_{i\nu\mu}$]. It also makes a convenient separation between gradients of p and gradients of R [Eq. (4.4)]:

$$(D_i\Sigma)_{0j}=(\partial_i\Sigma_{0\nu})\Sigma_{j\nu}-\kappa J_{i0j}=\kappa(\partial_i p_\nu R_{\nu j}-\delta_{ij})\ ,$$
$$(D_i\Sigma)_{jk}=(\partial_i\Sigma_{j\nu})\Sigma_{k\nu}-\kappa J_{ijk}=(\partial_i R_{\nu j})R_{\nu k}\ , \tag{5.15}$$
$$(D_i\Sigma)_{j0}=-(D_i\Sigma)_{0j}\ .$$

This covariant derivative cannot be made everywhere zero in a region of (physical flat) space, since its curvature is nonzero. [See Eq. (2.3) for the curvature of the blue-phase covariant derivative.] If one rolls the sphere around a small closed square (moving successively a distance ξ along $\hat{\mathbf{e}}_i$, $\hat{\mathbf{e}}_j$, $-\hat{\mathbf{e}}_i$ and $-\hat{\mathbf{e}}_j$) the original orientation Σ of the sphere changes to

$$[R_{-\xi\hat{e}_j}R_{-\xi\hat{e}_i}R_{\xi\hat{e}_j}R_{\xi\hat{e}_i}\Sigma]_{\mu\nu}=\kappa^2[J_i,J_j]_{\mu\rho}\Sigma_{\rho\nu}$$
$$=\mathscr{R}_{ij\mu\rho}\Sigma_{\rho\nu}\ , \tag{5.16}$$

where the curvature $\mathscr{R}$ is not zero:

$$\mathscr{R}_{ij\mu\nu}=\kappa^2[J_i,J_j]_{\mu\nu}=\kappa^2(\delta_{j\mu}\delta_{i\nu}-\delta_{i\mu}\delta_{j\nu})\ . \tag{5.17}$$

Thus $D\Sigma$ cannot be made zero along infinitesimal square loops, and thus can only vanish at points and along lines.

The simplest form for the metallic glass free-energy density (a "one-constant approximation") is given by summing the squares of the components of $D\Sigma$:

$$F\{\Sigma\}=\mathrm{Tr}(D_i\Sigma)^T(D_i\Sigma)=(D_i\Sigma)_{\mu\nu}(D_i\Sigma)_{\mu\nu}$$
$$=\kappa^2(\partial_i p_\nu R_{\nu j}-\delta_{ij})^2+(\partial_i R_{\nu j}R_{\nu k})^2\ . \tag{5.18}$$

This is the continuum elastic energy with which we propose to model the metallic glasses. It is frustrated; since $D\Sigma$ cannot be made zero in a volume, neither can F. This nonzero value represents the deformation energy needed

to pack the local tetrahedral clusters of atoms to fill physical space.

Further properties and more general forms of the metallic glass free energy (5.21) (which will not be useful to us here) are discussed in Appendix B. We turn now to study defect lines.

VI. DEFECT LINES AND THE CONTINUUM LIMIT

One problem with discussing defect lines within continuum field theories is the eventual necessity of studying the core of the defect. Since the strains diverge at the defect, linear elasticity breaks down and a more complete theory is necessary. Since the energy depends only logarithmically on the core radius (cutoff length), this study is not very rewarding. In this section we will develop an elegant method for avoiding the detailed study of defect cores. In the continuum limit, only the core energy per unit length will matter—all other properties of the core will be irrelevant.

The cores are clearly important in the blue phases and metallic glasses. First, the ground states have a finite density of defect lines. The magnitude of our order parameters is fixed. Near the defect lines we must either allow the magnitude to vary (as in Landau theory[11,12,1,13,31]), or put the theory on a lattice.[3] Secondly, the cutoff length is comparable to the distance between defects; there are two length scales in the problem. In the metallic glasses, the radius of curvature κ^{-1} is ~ 1.6 times the atomic diameter. In cholesterics, the core size must be on the order of the pitch[2,12] for the blue phases to be stable.

Are we being perverse in insisting on a fixed-magnitude order parameter to describe lattices of defects with large cores? It is possible that two length scales are necessary for describing these phases properly. However, it is certainly preferable to work in the continuum limit (neglecting the cores) if the essential physics can be left unchanged. (What things are essential—which properties if any are universal, and independent of the model used to describe the system—is not clear at this time.) For example, metallic glasses have been described using dense packings of spheres,[22,24] using a soft-spin Landau theory,[13,31] and using an SO(4) order parameter[10] with an explicit cutoff. Each theory treats the short-distance scales (the defect cores) differently. I assert that if these models share any common quantitative predictions about the real metallic glass state, it is because they share the same continuum limit.[47]

To take the continuum limit, we must somehow keep the energy per unit length of the defect lines fixed as the cutoff radius Λ is taken to zero. Briefly, we do this by adding a counterterm to the free energy—a total divergence whose net contribution is proportional to the length of the defect lines. As we let the cutoff Λ get small, we increase the magnitude of this counterterm so as to keep the defect energy fixed. (This is of course a renormalization-group transformation.) In the limit, we can study defect lines in a continuum theory without a cutoff. A term like this is well known in the study of singularity-free defects. (These codimension-zero defects are called variously instantons, textures, and "skyrmions.") There the term is purely topological. Its integral over all space is an integer (the wrapping number of the order parameter field) which counts the number of defects. The term we use works for a more subtle reason, since it needs both topology and energetics to measure the length of the defect lines.

First we give a complete analysis of the continuum limit for $s=-\frac{1}{2}$ lines in the blue phase (or more generally in any phase with a vector or director order parameter). In the continuum limit the counterterm will energetically constrain $\mathbf{n}$ to be perpendicular to the defect. With these boundary conditions the counterterm is a topological measure of the winding number of $\vec{\mathbf{n}}$ around the defect. The integral of the counterterm is proportional to the sum of the lengths of the defect lines multiplied by their strengths. Secondly, we will analyze a total divergence counterterm for SO(3) order parameters. Disclinations in these theories are important in themselves,[48] and they form a simpler analog of the metallic glass defects. In the continuum limit, the order parameter will be energetically constrained to rotate about an axis parallel to the defect. (This makes the counterterm energy stationary, but minimizes only the full free energy.) Again, with these boundary conditions the counterterm topologically measures the product of the strengths and lengths of the disclination lines. Finally, we give the form of the counterterm for the metallic glass order parameter, and sketch the continuum limit of 6-lines ($-72°$ disclinations).

Consider a defect line of length L in the blue phase. Let C be a cylinder of radius Λ about the defect (Fig. 20). The energy density we will use outside C is given by Eq. (5.10) plus a total divergence term:

$$F_\Lambda\{n\}=\tfrac{1}{2}K(\partial_i n_j+q\epsilon_{ijk}n_k)^2+\tfrac{1}{2}\bar{K}(\Lambda)\partial_i(n_j\partial_j n_i-n_i\partial_j n_j) \tag{6.1}$$

$$=\tfrac{1}{2}K\{(\mathrm{div}n)^2+(n\times\mathrm{curl}n)^2+(n\cdot\mathrm{curl}n+q)^2\}+\tfrac{1}{2}[K+\bar{K}(\Lambda)]\mathrm{div}(n\cdot\nabla n-n\nabla\cdot n)+\tfrac{1}{2}Kq^2\ . \tag{6.2}$$

The first term in curly brackets in Eq. (6.2) is a sum of squares, and is zero only for the helical phase (2.5). The second term is a total divergence, which can stabilize the blue phase only if the effective energy per unit length of the defect line is sufficiently negative.[2] We wish to define $\bar{K}(\Lambda)$ so as to keep the energy of an $s=-\frac{1}{2}$ defect line fixed as $\Lambda\to 0$.

We can make many simplifications by ignoring terms which change the energy per unit length by a finite amount. The bulk energy of the core $\sim\Lambda^2$, and vanishes with Λ. The isotropic blue-phase surface tension $\sigma=\alpha K/\xi$, where ξ is the width of the interface[38] and α is somewhat less than one.[49] As Λ goes to 0, $\xi\sim\Lambda$ so the interfacial energy $2\pi\Lambda\sigma$ goes to a constant. Terms involving the wave number of the pitch q are only linear in the gradients $\partial n\sim 1/r$ so their contributions will be finite as $\Lambda\to 0$. The effects of the radius of curvature r and the torsion t of the defect line are also higher order in Λ/r and Λt, respectively; thus we may assume the defect line is straight. Finally, the effects of the boundary condi-

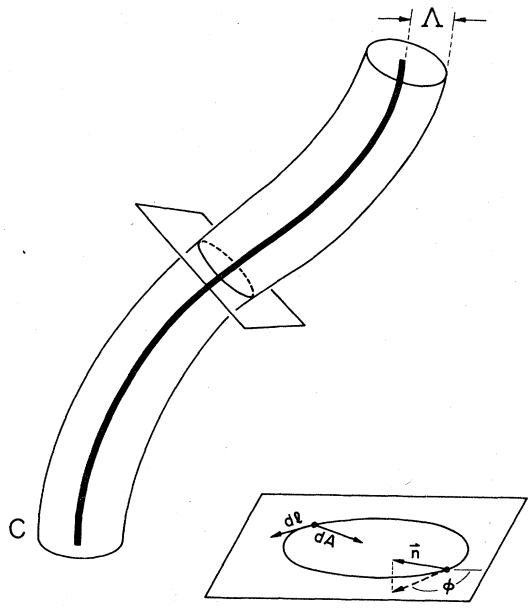

FIG. 20. *Core of defect line.* The cylinder C is of radius Λ about the defect line. The differential surface area $d\mathbf{A}$ points perpendicular to the cylinder, into it. Consider a plane perpendicular to the defect. The differential arclength dl measures length along the circular intersection of C with the plane; $\mathbf{dl}\cdot\mathbf{dA}=0$. The blue-phase order parameter $\vec{n}$, when projected onto the plane, makes an angle ϕ with respect to some fixed axis.

tions are down by Λ/R, where R is the distance to the boundary (e.g., to nearby defects), so apart from the total divergence $\bar{K}(\Lambda)$ (which we will treat explicitly as a surface term) the boundary too can be ignored. We are thus left with the problem of minimizing

$$F_\Lambda^0+S_\Lambda=\int_\Lambda \tfrac{1}{2}K(\partial_i n_j)^2 dV + \tfrac{1}{2}\bar{K}(\Lambda)\int_c (n\cdot\nabla n - n\nabla\cdot n)\cdot dA \tag{6.3}$$

in the vicinity of a straight defect of length L.

Assume the defect lies along the z axis. The first term contributes energy,

$$F_\Lambda^0=\tfrac{1}{2}K\int dz\int_\Lambda dr\int_0^{2\pi} d\theta\, r\left[\left[\frac{\partial n_i}{\partial z}\right]^2+\left[\frac{\partial n_i}{\partial r}\right]^2+\frac{1}{r^2}\left[\frac{\partial n_i}{\partial\theta}\right]^2\right], \tag{6.4}$$

where (because of the defect) $n(r,0,z)=-n(r,2\pi,z)$. Clearly $\partial n/\partial z=\partial n/\partial r=0$ for minimum energy; $\int_0^{2\pi}(\partial n_i/\partial\theta)^2 d\theta$ is stationary for $\partial^2 n_i/\partial\theta^2=s^2 n_i$, with $s=\pm\frac{1}{2},\pm\frac{3}{2},\ldots$. Since $n(2\pi)=-n(0)$, at some point $n_z(\theta)=0$, and without loss of generality we may assume $n_z(0)=0$ and $\mathbf{n}(0)=(1,0,0)$. Then the stationary solutions for F_Λ^0 are

$$n(\theta)=(\cos(s\theta),A\sin(s\theta),(1-A^2)^{1/2}\sin(s\theta)), \tag{6.5}$$

so n moves along great circles on the sphere $n^2=1$. Since $(\partial n/\partial\theta)^2=s^2$, the energy from F_Λ^0 is

$$F_\Lambda^0=\int_{-L/2}^{L/2}dz\int_\Lambda^R dr\frac{\pi K}{r}s^2=\pi KLs^2\ln(\Lambda^{-1}). \tag{6.6}$$

The second term S_Λ is the surface integral equaling (by Gauss's law) the total divergence term in Eq. (6.1). Project $\mathbf{n}$ onto the plane perpendicular to the defect and let ϕ be the angle between the projection and some fixed axis in the plane (Fig. 20). Here our defect lies along $\hat{\mathbf{z}}$, so we can let $\phi=\arctan(n_2/n_1)$. S_Λ can be reexpressed in terms of $\nabla\phi$:

$$\nabla\phi=\frac{1}{n_1^2+n_2^2}\begin{bmatrix}-n_2\partial_1 n_1+n_1\partial_1 n_2\\ -n_2\partial_2 n_1+n_1\partial_2 n_2\end{bmatrix}, \tag{6.7}$$

and the line element dl measuring arclength along the cylinder C is given by $(dl_x,dl_y)=(dA_y,-dA_x)$, so

$$(n_1^2+n_2^2)\nabla\phi\cdot dl=(n\cdot\nabla n-n\nabla\cdot n)\cdot dA. \tag{6.8}$$

Thus,

$$S_\Lambda=\tfrac{1}{2}\bar{K}(\Lambda)\int dz\int(1-n_3^2)\nabla\phi\cdot dl. \tag{6.9}$$

Notice two important features of S_Λ. First, if $n_3\equiv 0$, it measures the winding number of the defect:

$$s=(1/2\pi)\int\nabla\phi\cdot dl. \tag{6.10}$$

Secondly, if ϕ is monotone decreasing ($\bar{K}>0, s<0$) it is minimized by $n_3\equiv 0$, so minimizing S_Λ for negative winding numbers gives

$$S_\Lambda=\tfrac{1}{2}\bar{K}(\Lambda)(2\pi s)L=\pi s\bar{K}(\Lambda)L. \tag{6.11}$$

[Similarly, positive disclination ($s>0$) can be stabilized by negative $\bar{K}$.]

Thus for a given winding number s, F_Λ^0 and S_Λ can be simultaneously minimized by

$$n=(\cos(s\theta),-\sin(s\theta),0), \tag{6.12}$$

with energy per unit length

$$F_\Lambda^0+S_\Lambda=\pi L[Ks^2\ln(\Lambda^{-1})+\bar{K}(\Lambda)s].$$

To keep the energy per unit length of $s=-\frac{1}{2}$ defect lines fixed, we set

$$\bar{K}(\Lambda)=K_0+\tfrac{1}{2}K\ln\Lambda^{-1}. \tag{6.13}$$

The energy per unit length $(-\pi/2)K_0$ of the $s=-\frac{1}{2}$ defect will depend upon the shape of the defect line, the core and surface tension energies, and the position of neighboring defects. Energies of defects of all other winding numbers diverge as $\Lambda\to 0$; in the continuum limit only $s=-\frac{1}{2}$ defects are allowed.

We now consider defect lines in a theory with an SO(3) rotation matrix order parameter. Such a theory would describe, for example, a material with completely broken orientational order (three distinguished axes in space) but without translational order. Our primary motivation for this calculation is its similarity to the (conjectured) calculation for the SO(4) theory of metallic glasses. Even here, the detailed estimates use Euler angles and are confined to Appendix C.

Superfluid ^{3}He and biaxial nematics are described by SO(3) order parameters. The bulk free energies in these materials are more complicated than the one we will use, but one might be able to modify this calculation to treat defects in these materials. On long length scales, Heisenberg spin glasses are thought to be described by an SO(3) order parameter[48] (representing the local rotation needed to align two metastable states). However, wall defects as well as line defects appear to be important in the numerical simulations.

The free-energy density F is a sum of a bulk free energy which resists gradients in the order parameter R_{ij}, and a surface term:

$$F\{R\}=\tfrac{1}{2}K(\partial_i R_{jk})^2+\tfrac{1}{2}\bar{K}(\Lambda)\partial_j(R_{ik}\partial_k R_{ij}-R_{ij}\partial_k R_{ik}) . \tag{6.14}$$

Just as in the blue phase, we can confine our attention to a straight defect line in the $\hat{z}$ direction and assume all gradients are zero in the $\hat{r}$ and $\hat{z}$ directions. As one moves around the defect line $R(2\pi)$ must equal $R(0)$ followed by a symmetry g of the undistorted phase:[50] $R(2\pi)=gR(0)=e^{2\pi J}R(0)$.

The first term in F is locally minimized by a steady rotation,

$$R(\theta)=e^{J\theta}R(0) . \tag{6.15}$$

This gives

$$(\partial_i R_{jk})^2=1/r^2(J_{jk})^2=2s^2/r^2 ,$$

where s is the strength of the disclination g (the net angle rotated, divided by 2π). The bulk energy per unit length is thus $2\pi Ks^2\ln(\Lambda^{-1})$.

The second term is again a total divergence, which we will express as a surface integral. Let $W_j=R_{ik}\partial_k R_{ij}-R_{ij}\partial_k R_{ik}$; then just as in the blue phase

$$\int_\Lambda dV\,\mathrm{div}W=\int_c W\cdot dA=L\int dl_i\,\epsilon_{ij3}W_j . \tag{6.16}$$

For the moment, we assume that $R(\theta)$ satisfies (6.15) (minimizes the bulk free energy). We will show in Appendix C that this solution is a local minimum of the free energy (6.14). Define $\mathbf{m}$ by

$$(R^{-1}\partial_k R)_{ij}=R(0)_{li}J_{lm}R(0)_{mj}\partial_k\theta=m_l\epsilon_{ijl}\partial_k\theta ;$$

$\hat{\mathbf{m}}$ is the axis in physical space about which the order parameter rotates and $m^2=s^2$. The energy per unit length contributed by the surface term is

$$\frac{\bar{K}(\Lambda)}{2}\int dl_i\,\epsilon_{ij3}(\epsilon_{kjl}-\epsilon_{jkl})m_l\partial_k\theta=2\pi\bar{K}(\Lambda)m_3 . \tag{6.17}$$

Thus the surface term is made most negative (for $\bar{K}>0, s<0$) with $\mathbf{m}=s\hat{\mathbf{z}}$; one can always choose $R(0)$ to align the axis of rotation with the defect line. Setting

$$\bar{K}(\Lambda)=K_0-Ks\ln\Lambda^{-1} \tag{6.18}$$

gives the disclination of strength s a smooth continuum limit, with core energy $2\pi K_0 s$ per unit length.

Finally, we consider disclination lines in our SO(4) theory of metallic glasses. We add a total divergence to the metallic glass free energy (5.21):

$$F\{\Sigma\}=\tfrac{1}{2}K(D_i\Sigma)^2_{\mu\nu}+\tfrac{1}{2}\bar{K}(\Lambda)\partial_j[(\Sigma\partial_k\Sigma^{-1})_{kj}-(\Sigma\partial_k\Sigma^{-1})_{jk}] \tag{6.19}$$

$$=\tfrac{1}{2}K[\kappa^2(\partial_i p_\nu R_{\nu j}-\delta_{ij})^2+(\partial_i R_{\nu j}R_{\nu k})^2]+\tfrac{1}{2}\bar{K}(\Lambda)\partial_j(R_{\nu k}\partial_k R_{\nu j}-R_{\nu j}\partial_k R_{\nu k}) . \tag{6.20}$$

Again we need only consider straight defects, symmetric in $\hat{z}$ and $\hat{r}$. Also, as in the blue phase, we can ignore the terms linear in the gradients (which embody the frustration), so in (6.19) we may replace D_i by ∂_i when studying defect cores. We want to minimize $F\{\Sigma\}$ subject to the constraint that $\Sigma(2\pi)=\Sigma(0)g=\Sigma(0)e^{2\pi J}$, where g is a symmetry of the ideal template.

The bulk energy (ignoring the frustration) is locally minimized by

$$\Sigma(\theta)=\Sigma(0)e^{J\theta}=e^{\tilde{J}\theta}\Sigma(0) . \tag{6.21}$$

$\tilde{J}=\Sigma(0)J\Sigma^{-1}(0)$ represents the infinitesimal rotation of the ideal template as θ revolves around the disclination line. Just as in (6.15),

$$(\partial_i\Sigma_{\mu\nu})^2=\frac{(J_{\mu\nu})^2}{r^2}=\frac{(\tilde{J}_{\mu\nu})^2}{r^2}=\frac{2s^2}{r^2} ,$$

where s is the strength of the disclination.

We will assume that the minimum energy defect is of the form (6.21). [The demonstration of this should be similar to the SO(3) calculation given in Appendix C.] If we define

$$W_j=(\Sigma\partial_k\Sigma^{-1})_{kj}-(\Sigma\partial_k\Sigma^{-1})_{jk}=2\tilde{J}_{kj}\partial_k\theta ,$$

then

$$\int_\Lambda dV\,\mathrm{div}W=L\int dl_i\,\epsilon_{ij3}W_j$$

$$=2L\epsilon_{123}\tilde{J}_{12}\int\nabla\theta\cdot dl=4\pi L\tilde{J}_{12} . \tag{6.22}$$

Since $(\tilde{J}_{ij})^2=2s^2$, the surface term (for negative s) is minimized by $\tilde{J}_{12}=-\tilde{J}_{21}=s$ and $\tilde{J}_{ij}$ otherwise zero. Thus,

$$\Sigma(\theta)=\begin{bmatrix}1&0&0&0\\0&\cos(s\theta)&\sin(s\theta)&0\\0&-\sin(s\theta)&\cos(s\theta)&0\\0&0&0&1\end{bmatrix}\Sigma(0) . \tag{6.23}$$

This minimum energy defect is an orientational defect only; the position p_ν on the ideal template is independent of θ near the core:

$$p_\nu(\theta)=\Sigma_{0\nu}(\theta)=[e^{\tilde{J}\theta}]_{0\rho}\Sigma_{\rho\nu}(0)=p_\nu(0) . \tag{6.24}$$

It also rotates about an axis parallel to the defect ($\hat{z}$). Setting

$$\bar{K}(\Lambda)=K_0-Ks\ln\Lambda^{-1} \tag{6.25}$$

with $s=-\frac{1}{5}$ for the metallic glasses gives the sixfold coordinated edge defects a smooth continuum limit with

core energy $-2\pi K_0/5$ per unit length.

In summary, the strain energy near defect lines diverges logarithmically as the cutoff length (core size) goes to zero. To compensate, we can add a total divergence to the free energy, which cannot change the bulk energies of defect-free phases, since it can be written as a surface integral. However, in the phases of interest there is a lattice of defect lines, and therefore a finite density of internal surface area per unit volume. We allow the magnitude of this total divergence term to diverge as the cutoff gets small, in order to keep the net energy per unit length of the defects finite. In this limit, the divergence term enforces boundary conditions at the singularity. With these boundary conditions, the total divergence is a topological measure of the winding number of the defects. In the continuum limit, the minimum strength disclination lines have finite energy per unit length; all other defect lines are energetically forbidden.

ACKNOWLEDGMENTS

I would like to thank David Wright, David DiVincenzo, and David Mermin for careful readings of the manuscript and David Nelson for many provoking questions and helpful suggestions. Thanks are also due to Doug Eardley and Frank Wilczek for useful discussions. This work was supported by National Science Foundation Grant No. PHY-77-27084.

APPENDIX A: BLUE-PHASE COVARIANT DERIVATIVE

We have defined the order parameter to be the orientation of the spherical template needed to match the environments at the point of tangency to physical space. We define the covariant derivative by rolling the sphere along physical space without slipping (Fig. 18). To roll the sphere a small distance $\xi=\xi_1\hat{\mathbf{e}}_1+\xi_2\hat{\mathbf{e}}_2+\xi_3\hat{\mathbf{e}}_3$, one uses the rotation

$$\Sigma_\xi=\exp(q\xi_i J_i)\simeq\mathbb{1}+q\xi_i J_i \ ,$$

where $(J_i)_{\mu\nu}$ is defined in Eq. (5.12). The local state at a point $\mathbf{r}$ is given by the set of rotations Σ satisfying

$$n(\mathbf{r})=\tilde{\Sigma}n^I(\tilde{\Sigma}^{-1}\hat{x}_0) \ , \tag{A1}$$

and which thereby align n^I at the top of the sphere $\hat{x}_0$ with $\mathbf{n}(r)$. The ideal low-energy state for $r+\xi$ is given by first aligning the template to r using $\tilde{\Sigma}$ and then rolling it to $r+\xi$. This defines a parallel-transported rotation field $\tilde{\Sigma}^{\rm PT}$,

$$[\tilde{\Sigma}^{\rm PT}(\mathbf{r}+\boldsymbol{\xi})]=\Sigma_\xi\tilde{\Sigma}(\mathbf{r}) \ , \tag{A2}$$

which gives a parallel-transported order parameter field,

$$\begin{aligned} n^{\rm PT}(\mathbf{r}+\boldsymbol{\xi})&=\Sigma_\xi\tilde{\Sigma}n^I(\tilde{\Sigma}^{-1}\Sigma_\xi^{-1}\hat{x}_0) \\ &\simeq n_\mu(\mathbf{r})+\xi_i[\,qJ_{i\mu\lambda}\tilde{\Sigma}_{\lambda\nu}n^I_\nu(\tilde{\Sigma}^{-1}\hat{x}_0) \\ &\quad -\tilde{\Sigma}_{\mu\nu}\partial_\sigma n^I_\nu\Sigma_{\tau\sigma}J_{i\tau 0}] \ . \end{aligned} \tag{A3}$$

Using the identities $n^I_\nu(p)=\partial_\sigma n^I_\nu p_\sigma$ and $\partial_\sigma n^I_\nu=-\partial_\nu n^I_\sigma$, we can write the covariant derivative:

$$\begin{aligned} (D_i n)_j&=\partial_i n_j-\lim_{\xi\to 0}\frac{n_j^{\rm PT}(\mathbf{r}+\xi\hat{e}_i)-n_j(r)}{\xi} \\ &=\partial_i n_j+[J_i,\tilde{\Sigma}(\partial n^I)\tilde{\Sigma}^{-1}]_{j0} \ . \end{aligned} \tag{A4}$$

Since ∂n^I [cf. Eq. (5.8)] generates an infinitesimal right-handed rotation, we have expressed the blue-phase covariant derivative in terms of commutators of generators of SO(4), i.e., in terms of the structure constants of the group.

To evaluate this commutator, we introduce a basis for the infinitesimal generators.[17] The six generators of SO(4) split naturally into right- and left-handed groups of three, J_i^R and J_i^L:

$$J_1^R=\begin{bmatrix} 0&1&0&0\\ -1&0&0&0\\ 0&0&0&-1\\ 0&0&1&0 \end{bmatrix},\quad J_2^R=\begin{bmatrix} 0&0&1&0\\ 0&0&0&1\\ -1&0&0&0\\ 0&-1&0&0 \end{bmatrix},\quad J_3^R=\begin{bmatrix} 0&0&0&1\\ 0&0&-1&0\\ 0&1&0&0\\ -1&0&0&0 \end{bmatrix},$$

$$J_1^L=\begin{bmatrix} 0&1&0&0\\ -1&0&0&0\\ 0&0&0&1\\ 0&0&-1&0 \end{bmatrix},\quad J_2^L=\begin{bmatrix} 0&0&1&0\\ 0&0&0&-1\\ -1&0&0&0\\ 0&1&0&0 \end{bmatrix},\quad J_3^L=\begin{bmatrix} 0&0&0&1\\ 0&0&1&0\\ 0&-1&0&0\\ -1&0&0&0 \end{bmatrix}.$$

Thus from Eq. (5.12) $J_i=(J_i^R+J_i^L)/2$. Each set has the commutation relations of the three dimensional rotations: $[J_i^R,J_j^R]=2\epsilon_{ijk}J_k^R$ and $[J_i^L,J_j^L]=2\epsilon_{ijk}J_k^L$; also $[J_i^R,J_j^L]=0$. Thus locally, SO(4) looks like a direct product $SO_R(3)\otimes SO_L(3)$.

Now, $\tilde{\Sigma}\partial\cdot n^I\tilde{\Sigma}^{-1}=q\tilde{\Sigma}J_1^R\tilde{\Sigma}^{-1}$ is a right-handed infinitesimal rotation, so it can be written as a linear combination of the J_i^R. Since

$$n_j(r)=\tilde{\Sigma}n^I(\tilde{\Sigma}^{-1}(\hat{x}_0))=\tilde{\Sigma}_{j\nu}\partial_\sigma n^I_\nu\tilde{\Sigma}_{0\sigma}=(\tilde{\Sigma}\partial n^I\tilde{\Sigma}^{-1})_{0j}$$

and $(J_i)_{0j}=\delta_{ij}$, $\tilde{\Sigma}\partial n^I\tilde{\Sigma}^{-1}=n_iJ_i^R$. Rolling the sphere in a direction $\hat{e}_i$ is generated by $J_i=(J_i^R+J_i^L)/2$ [Eq. (5.10)], so

$$\begin{aligned} [J_i,\tilde{\Sigma}\partial n^I\tilde{\Sigma}^{-1}]_{j0}&=(q/2)[J_i^R,n_kJ_k^R]_{j0}=q\epsilon_{ikm}n_kJ^R_{mj0} \\ &=+q\epsilon_{ijk}n_k \ , \end{aligned} \tag{A5}$$

and the definition (5.9) of the covariant derivative is obtained. Thus, the local low-energy blue-phase state is con-

structed by rolling the ideal template infinitesimal distances on physical space.[17]

APPENDIX B: METALLIC GLASS FREE ENERGY

In this appendix we discuss the gauge invariances and flat-space limit of the metallic glass free energy (5.21).

The gauge invariance of the metallic glass free energy corresponds to the arbitrary choice of the point of tangency $\hat{x}_0$ and the arbitrary orientation of physical space at $\hat{x}_0$. Let $\Omega(r)\in SO(4)$ describe the local gauge transformation

$$\Sigma^* = \Omega\Sigma ,$$
$$J_i^* = \Omega J_i \Omega^{-1} + \frac{1}{\kappa}(\partial_i \Omega)\Omega^{-1} . \tag{B1}$$

Then

$$\begin{aligned} D_i^*(\Sigma^*) &= (\partial_i \Sigma^*)\Sigma^{*-1} - \kappa J_i^* \\ &= (\partial_i \Omega)\Omega^{-1} + \Omega(\partial_i \Sigma)\Sigma^{-1}\Omega^{-1} \\ &\quad - \kappa[\Omega J_i \Omega^{-1} + (1/\kappa)(\partial_i \Omega)\Omega^{-1}] \\ &= \Omega[(\partial_i \Sigma)\Sigma^{-1} - \kappa J_i]\Omega^{-1} \\ &= \Omega(D_i \Sigma)\Omega^{-1} , \end{aligned} \tag{B2}$$

and F in Eq. (5.21) is unchanged.

Now we investigate the flat-space limit $\kappa \to 0$. First, we must generalize the free energy by giving the two terms of $F\{\Sigma\}$ separate elastic constants:

$$F\{\Sigma\} = \tfrac{1}{2}K_p(\partial_i p_\nu R_{\nu j} - \delta_{ij})^2 + \tfrac{1}{2}K_R(\partial_i R_{\nu j} R_{\nu j})^2 . \tag{B3}$$

[We can use $\hat{x}_0$ and $\bar{\delta}_{\mu\nu} = \delta_{\mu\nu} - (\hat{x}_0)_\mu (\hat{x}_0)_\nu$ to form more general free energies; gradients of p and of r are physically distinct.] If we set $p(\mathbf{r}=\mathbf{0}) = \hat{x}_0$, then as $\kappa \to 0$ we can write $p = (\kappa^{-1}, \mathbf{p})$; also

$$R_{0j} = \kappa R_{\nu j} p_\nu = \Sigma_{j\nu}\Sigma_{0\nu} = \delta_{0j} = 0 ,$$

so R_{jk} is a 3×3 rotation matrix. Thus,

$$\lim_{\kappa\to 0} \tilde{F}(\Sigma) = \tfrac{1}{2}K_p(\partial_i p_k R_{kj} - \delta_{ij})^2 + \tfrac{1}{2}K_R(\partial_i R_{jk})^2 . \tag{B4}$$

Changing the sign inside the first term and conjugating it by R leads us finally to the form

$$\lim_{\kappa\to 0} F^*(\Sigma) = \tfrac{1}{2}K_p(\delta_{ij} - R_{ik}\partial_k p_j)^2 + \tfrac{1}{2}K_R(\partial_i R_{jk})^2 . \tag{B5}$$

The first term is precisely the square of the strain matrix e_{ij} of Eq. (5.6); we simply identify $\frac{1}{2}K_p$ in (B5) with 2μ in (5.7). The second term does not occur in flat-space continuum elastic theory. It is allowed by symmetry, but since R is implicitly defined from gradients $\partial_i p_j$ of p, gradients of R are second derivatives of p. Second derivatives contribute energies of higher order in the lattice constant over the wavelength. Continuum elastic theory is normally concerned with wavelengths that are long compared to the lattice constant a, and higher-order terms can be dropped. We are interested in strains on length scales $\kappa^{-1} \sim 1.6a$, and must be careful to keep whatever higher-order gradient terms appear important.

APPENDIX C: STABILITY OF SO(3) DISCLINATION CORES

In Sec. VI, we analyzed the energy of a disclination in an SO(3) order parameter field $R(\theta)$, assuming that the core structure was of the form (6.15) which minimizes the bulk free energy. Since the surface term is by hand kept comparable to the bulk contributions (to keep the net energy finite), we must check that this form remains a local minimum of the full free energy.

In the blue phase, this was obvious; the simple form (6.9) for the surface energy makes it obvious that the bulk and surface energies are simultaneously globally minimized by (6.12). We will do a local stability analysis for SO(3).

Let $(L_i)_{jk} = \epsilon_{ijk}$ be the generators of rotations in SO(3). Express R in Euler angles (ϕ,ξ,ψ):

$$R = e^{\phi L_3} e^{\xi L_1} e^{\psi L_3} . \tag{C1}$$

Then one can show[51]

$$\begin{aligned} R^{-1}\nabla_k R = &[(\sin\psi)(\sin\xi)\partial_k\phi + (\cos\psi)\partial_k\xi]L_1 \\ &+ [(\cos\psi)(\sin\xi)\partial_k\phi - (\sin\psi)\partial_k\xi]L_2 \\ &+ [(\cos\xi)\partial_k\phi + \partial_k\psi]L_3 , \end{aligned} \tag{C2}$$

and

$$\epsilon_{ij3}W_j = 2[(\cos\xi)\partial_i\phi + \partial_i\psi] . \tag{C3}$$

The surface term energy per unit length

$$\tfrac{1}{2}\bar{K}(\Lambda)\int dl_i\, \epsilon_{ij3}W_j = \bar{K}(\Lambda)\int [(\cos\xi)\nabla\phi + \nabla\psi]\cdot dl \tag{C4}$$

is stationary only for $R(\theta)$ with ψ arbitrary but ξ and ϕ constant; thus

$$R(\theta) = R_0 e^{\psi L_3} . \tag{C5}$$

Thus the condition that the surface term be stationary fixes the axis of rotation parallel to the defect [cf. (6.17)], and with this boundary condition, the surface term is $K(\Lambda)$ times $\int \nabla\psi\cdot dl = 2\pi s$ independent of $\psi(\theta)$; it topologically measures the strength of the disclination.

However, the surface term is *not* minimized by the form (C5) (unlike the blue phase). We must perform a second variation of the full free energy to determine local stability.

The bulk free energy per unit length is given by the square of (C2):

$$\begin{aligned} &\int_\Lambda dr \int_0^{2\pi} d\theta\, r\tfrac{1}{2}K(R^{-1}\nabla_k R)^2 \\ &\quad = (K\ln\Lambda^{-1})\int [(\partial_\theta\phi)^2 + (\partial_\theta\xi)^2 + (\partial_\theta\psi)^2 + 2(\cos\xi) \\ &\qquad \times(\partial_\theta\phi)(\partial_\theta\psi)]d\theta . \end{aligned} \tag{C6}$$

Using the scaling form (6.18) for $\bar{K}(\Lambda)$ (and dropping K_0) the total energy per unit length is

$$\begin{aligned} F = (K\ln\Lambda^{-1})\int d\theta\{ &(\partial_\theta\phi)^2 + (\partial_\theta\xi)^2 + (\partial_\theta\psi)^2 \\ &+ 2\cos\xi(\partial_\theta\phi)(\partial_\theta\psi) \\ &- s[(\cos\xi)\partial_\theta\phi + \partial_\theta\psi]\} . \end{aligned} \tag{C7}$$

We perturb F about the solution which minimizes the bulk term (6.15) and extremizes the surface term (C5):

$$(\phi,\xi,\psi)=(\phi_0+\epsilon_1,\xi_0+\epsilon_2,\psi_0+s\theta+\epsilon_3) \tag{C8}$$

where $\epsilon(0)=\epsilon(2\pi)=0$. Expanding (C7) to second order in ϵ, and noticing that $\int \partial_\theta \epsilon d\theta=0$, we find

$$F_{\epsilon^2}=K\ln\Lambda^{-1}\int d\theta\left[\frac{(1+\cos\xi_0)}{2}\left[\nabla\epsilon_1+\nabla\epsilon_3-\frac{s\sin\xi_0}{2(1+\cos\xi_0)}\epsilon_2^*\right]^2\right.$$
$$+\frac{(1-\cos\xi_0)}{2}\left[\nabla\epsilon_1-\nabla\epsilon_3-\frac{s\sin\xi_0}{2(1-\cos\xi_0)}\epsilon_2^*\right]^2$$
$$\left.+\nabla\epsilon_2^2-\frac{s^2\sin^2\xi_0}{8}\left[\frac{1}{1+\cos\xi_0}+\frac{1}{1-\cos\xi_0}\right](\epsilon_2^*)^2\right]. \tag{C8}$$

$$F_{\epsilon^2}=K\ln\Lambda^{-1}\int d\theta[(\partial_\theta\epsilon)^2+2\cos\xi_0(\partial_\theta\epsilon_1)(\partial_\theta\epsilon_3)$$
$$-\sin\xi_0(\partial_\theta\epsilon_1)\epsilon_2 s]. \tag{C9}$$

We can rewrite F in a less compact but more useful way. Let $\epsilon_2^*=\epsilon_2-1/2\pi\int\epsilon_2 d\theta$. Then

The first two terms in (C10) are positive definite and can be made zero by suitable choices of $\nabla\epsilon_1$ and $\nabla\epsilon_3$. Thus given ϵ_2 and minimizing with respect to ϵ_1 and ϵ_3, gives

$$F_{\epsilon^2}=(K\ln\Lambda^{-1})\int d\theta\left[(\nabla\epsilon_2)^2-\frac{s^2\sin\xi_0^2}{8}\left[\frac{2}{1-\cos^2\xi_0}\right](\epsilon_2^*)^2\right]=(K\ln\Lambda^{-1})\int_0^{2\pi}d\theta\left[(\nabla\epsilon_2)^2-\frac{s^2}{4}(\epsilon_2^*)^2\right],$$

which is positive definite for $|s|<2$.

*Permanent address.

[1]D. Wright and N. D. Mermin (unpublished) will review experimental and theoretical work on the blue phases.

[2]S. Meiboom, J. P. Sethna, P. W. Anderson, and W. F. Brinkman, Phys. Rev. Lett. **46**, 1216 (1981); **46**, 1656(E) (1981).

[3]S. Meiboom, M. Sammon, and W. F. Brinkman, Phys. Rev. A **27**, 438 (1983).

[4]F. C. Frank and J. S. Kasper, Acta Crystallogr. **11**, 184 (1958); **12**, 483 (1959).

[5]M. Kléman, J. Phys. (Paris) **43**, 1389 (1982).

[6]D. R. Nelson, Phys. Rev. Lett. **50**, 982 (1983); Phys. Rev. B **28**, 5515 (1983).

[7]A. Tardieu and J. Billard, J. Phys. (Paris) Colloq. **37**, C3-79 (1976).

[8]V. Luzzati and P. A. Spegt, Nature (London) **215**, 701 (1967).

[9]A. A. Abrikosov, Zh. Eksp. Teor. Fiz. **32**, 1442 (1957) [Sov. Phys.—JETP **5**, 1174 (1957)].

[10]J. P. Sethna, Phys. Rev. Lett. **51**, 2198 (1983).

[11]S. A. Brazovskii and S. G. Dmitriev, Zh. Eksp. Teor. Fiz. **69**, 979 (1975) [Sov. Phys.—JETP **42**, 497 (1975)].

[12]R. M. Hornreich and S. Shtrikman, J. Phys. (Paris) **41**, 335 (1980); Phys. Lett. **84A**, 20 (1981); and H. Grebel, R. M. Hornreich, and S. Shtrikman, Phys. Rev. A **28**, 1114 (1983).

[13]D. R. Nelson and M. Widom, Nucl. Phys. B **240**, 113 (1984).

[14]J. F. Sadoc, J. Dixmier, and A. Guinier, J. Non-Cryst. Solids **12**, 46 (1973).

[15]M. Kléman and J. F. Sadoc, J. Phys. (Paris) Lett. **40**, L569 (1979).

[16]H. S. M. Coxeter, *Introduction to Geometry* (Wiley, New York, 1969); *Regular Polytopes* (Dover, New York, 1973); Ill. J. Math. **2**, 746 (1958).

[17]J. P. Sethna, D. C. Wright, and N. D. Mermin, Phys. Rev. Lett. **51**, 467 (1983).

[18]P. W. Anderson, in *Ill Condensed Matter, Proceedings of the Les Houches Summer School, Session XXXI,* edited by R. Balian, R. Maynard, and G. Toulouse (North-Holland, Amsterdam, 1979).

[19]D. R. Nelson (private communication). Isolated disclination lines cannot cross, since the first homotopy group of the metallic glass order parameter space is non-Abelian.

[20]G. Toulouse, Commun. Phys. **2**, 115 (1977).

[21]C. W. Misner, K. S. Thorne, and J. A. Wheeler, *Gravitation* (Freeman, San Francisco, 1973), p. 340; S. Weinberg, *Gravitation and Cosmology* (Wiley, New York, 1972), p. 143.

[22]P. Chaudhari and D. Turnbull, Science **199**, 11 (1978).

[23]A. Rahman, J. Chem. Phys. **45**, 2585 (1966).

[24]F. Spaepen, in *Physics of Defects, Proceedings of the Les Houches Summer School, Session XXXV,* edited by R. Balian, M. Kléman, and J.-P. Poirier (North-Holland, Amsterdam, 1981).

[25]J. C. Phillips has been particularly skeptical about some of the models for metallic and covalent glasses. He does believe in local low-energy regions [Phys. Rev. B **24**, 1744 (1981)], but they are large (20—30 Å) and separated by surfaces.

[26]S. R. Nagel, Adv. Chem. Phys. **51**, 227 (1982).

[27]F. C. Frank, Proc. R. Soc. London, Ser. A **215**, 43 (1952).

[28]P. G. deGennes, *The Physics of Liquid Crystals* (Clarendon, Oxford, 1975).

[29]E. Schödinger, *Space-Time Structure* (Cambridge University Press, Cambridge, 1950).

[30]P. L. Finn and P. E. Cladis, Mol. Cryst. Liq. Cryst. **84**, 159 (1982).

[31]S. Sachdev and D. R. Nelson, Phys. Rev. Lett. **53**, 1947 (1984).

[32]R. M. Hornreich and S. Shtrikman, Phys. Rev. A **28**, 1791 (1983).

[33]The semicolon denotes covariant derivative with the standard (torsion-free) connection. The symbol ϵ_{ijk} is totally antisym-

metric in any orthonormal coordinate system for the tangent space.

[34]This template (3.1) has something to do with the mixmaster theory of the universe (Ref. 21). It arises naturally from the identification of the manifold S^3 with the [topologically equivalent group SU(2)]. Right-handed blue-phase templates are formed by multiplying elements of S^3 on the right by infinitesimal generators in su(2) [John Bagger (private communication); see also Ref. 35)].

[35]W. Miller, *Symmetry Groups and Their Applications* (Academic, New York, 1972), p. 223.

[36]D. P. DiVincenzo (private communication).

[37]This section is rather technical, and less interesting than the others. Equation (4.4) is the main conclusion of the section.

[38]B. I. Halperin and D. R. Nelson (private communication).

[39]P. J. Steinhardt, D. R. Nelson, and M. Ronchetti, Phys. Rev. Lett. **47**, 1297 (1981).

[40]N. D. Mermin, Rev. Mod. Phys. **51**, 591 (1979).

[41]We have used a director throughout this paper to describe the blue phase. However, in principle the quotient group of SO(4) by the template symmetries could have been different; the fact that we described the template using a director field did not prejudge the result. In particular, the minimum-energy state within Landau theory (quadrupolar order parameter) has the same symmetry (Ref. 17), and would also have led to a director description of the broken symmetry.

[42]This is not the traditional way of forming the free energy (Ref. 28). Typically one contracts the order parameter and its gradients to form all scalars of linear and quadratic order in the gradients. This leads to free energies with many elastic constants, and hides the physics of flattening the ideal templates. For example, a total divergence term in the cholesteric free energy, happily discarded in earlier treatments, will turn out in the next section to be central to understanding the blue phase (Ref. 2). It is only when covariant derivatives are used to express the free energy that the magnitude and importance of this term become apparent.

[43]R. P. Feynman, R. B. Leighton, and M. Sands, *The Feynman Lectures on Physics* (Addison-Wesley, Reading, 1964), Vol. II.

[44]L. D. Landau and E. M. Lifshitz, *Theory of Elasticity* (translated by J. B. Sykes and W. H. Reid) (Pergamon, Oxford, 1959), p. 2.

[45]In particular, if $\mu=0$ then a bulk expansion costs no energy. If $\partial_k p_i = B\delta_{ki}$ with $B>1$, then by choosing R to be a rotation by $\theta=\arccos(B^{-1})$, we can make F of Eq. (5.7) equal $\lambda(3-BR_{ii})^2=0$. The corresponding strain matrix $e_{ij}=\delta_{ij}-BR_{ij}$ is not symmetric.

[46]D. C. Wright, Ph.D. thesis, Cornell University, 1983, Appendix *G*. It appears that the cholesteric helical pitch and the double twist pitch are not always the same.

[47]I am being unavoidably vague about the "essential physics" that should be contained in these models; our theoretical understanding of these materials is still too primitive to know what features are important. This paper attempts to develop a tractable model for the metallic glasses. We can hope that this model will predict universal glass transition or low-frequency properties, but there is no evidence yet even for a glass transition in the theory. The various theories of metallic glasses are distinguished primarily in that they make different uncontrolled approximations on the atomic scale. If their predictions are to apply quantitatively to the real world, these approximations must be unimportant. The motivation for this section is to make this nebulous idea precise. The properties which are independent of cutoff are those which are preserved in the continuum limit; the continuum limit is the fixed point of my renormalization group; the metallic glass models will describe the real world quantitatively only if they share the same renormalization-group fixed point.

[48]C. Henley, Ann. Phys. **156**, 368 (1984); **156**, 324 (1984).

[49]For example, if we allow n to vary in magnitude in Eq. (6.1) and (inspired by Landau theory) we let $K(n)\sim n^2$, α will equal $\frac{1}{8}$ for a flat interface. If we include the Landau bulk free energy, α will increase further; if we allow biaxiality α will decrease somewhat.

[50]Here we interpret R_{ij} as analogous to R_{vj} in the metallic glasses—that rotation of *physical* space that aligns it to the *ideal* template. $\Sigma_{\mu\nu}$ rotates the ideal template, and so the equivalence classes are formed by multiplying ϵ on the other (right) side by g [Eq. (4.5)].

[51]W. Miller, *Symmetry Groups and Their Applications,* Ref. 35, p. 226.